37
36

FREE VIBRATIONS OF INFLATABLE DAMS

by

Jen-Chi Hsieh

Dissertation submitted to the Faculty of the
Virginia Polytechnic Institute and State University
in partial fulfillment of the requirements for the degree of
Doctor of Philosophy
in
Civil Engineering

APPROVED:

Raymond H. Plaut, Chairman

Dean T. Mook

Richard M. Barker

Kamal B. Rojiani

Eric R. Johnson

April, 1988

Blacksburg, Virginia

FREE VIBRATIONS OF INFLATABLE DAMS

by

Jen-Chi Hsieh

Raymond H. Plaut, Chairman

Civil Engineering

(ABSTRACT)

This work deals with the linear two-dimensional free vibrations of an inflated cylindrical membrane. An air-inflated membrane is considered first. Vibration frequencies and modes are determined for various cases. The lowest mode shape is anti-symmetric. In the rest of the work, the membrane is inflated with water. In some cases there is a reservoir of water on one side of the membrane. The membrane equation of motion is solved using a finite difference method, and the hydrodynamic pressures on the membrane, caused by the motion of the internal and external water domains, are treated by the boundary element method. The effects of the membrane parameters, internal and external water head, and density of the membrane on the lowest four frequencies are illustrated. For the membrane without the outside water, the first two natural frequencies agree well with experimental values. The existence of the upstream head has a significant influence on the frequencies, and the mode shapes are shown to be tilted toward the downstream side of the membrane.

Acknowledgements

I gratefully appreciate the guidance and encouragement of those people who have helped in various ways to complete this dissertation. I am especially thankful to Dr. Plaut for his direction and patience towards me in so many ways during the course of research; his kindness and continuous encouragement have made this research possible. I also want to thank Dr. Mook, who has guided me in the field of ideal fluid flows. Gratitude is also extended to Dr. Barker, Dr. Rojiani, and Dr. Johnson for serving as members of my degree committee. This research was sponsored by a grant from the National Science Foundation. Finally, I wish to thank my family for their understanding and support.

Table of Contents

List of Illustrations

List of Tables

Chapter 1

INTRODUCTION

1.1 Purpose and Scope

In this dissertation, the free vibrations of an inflatable cylindrical membrane dam which is filled with water are investigated. Most previous studies have only considered hydrostatic conditions. Few papers have treated the vibrational characteristics of the membrane, although two of these dams have failed, which may have been caused by excessive hydrodynamic forces. This aspect is studied by looking into the linear free vibrations, including the hydrodynamic effect, in a two-dimensional analysis.

The natural frequencies and the respective modes of vibrations are essential knowledge for further investigations on forced vibrations, which involve overflow conditions, wave forces and earthquakes. The purpose of this study is to provide research on this problem and facilitate the correct design of the inflatable membrane.

Since the interaction between the membrane and water is complex, in this dissertation we make the following simplifying assumptions:

1. The membrane structure is sufficiently long, so that a two-dimensional model of a section is appropriate.
2. The effect of damping on membrane vibrations is neglected.
3. The water is incompressible and inviscid.
4. The hydrodynamic pressures act on the membrane in the normal direction only.
5. The elongation of the membrane during vibrations is ignored.
6. The dynamic deflection of the membrane is small; therefore, a linear analysis is possible.

A fabric membrane has been used widely in various industries. Without inflation, it is useful as a storage bag for grains or explosive materials [1], and in other applications. Upon inflation, it can be used as a structure or as a temporary support for construction. Here a membrane dam pressurized by water is primarily studied, though it can also be pressurized by air, or a combination of water and air.

Inflatable dams have been constructed around the world. Of late, more than 100 membrane dams are being built in China alone, as water-impounding devices for flood control and the diversion of streams. In addition, these dams can have the function of storing some of the water in the rainy season for later farming uses. Features of applications of some dams already installed in the United States are shown in Table 1.1. The membrane dam is especially economical and easily constructed when compared to traditional concrete dams. Using it may cut the cost of construction up to 60%. Recent advanced techniques also help the fabric material of the membrane to achieve higher durability.

Some investigations have been carried out to find the static shape of the membrane dam under various loading conditions, but the collapse of a water-inflated dam in Pakistan, in 1967 [2], and of a water-and-air-inflated dam in Australia, in 1969 [3], show the necessity to study the dynamic behavior of the membrane dam.

It is anticipated that similar dynamic characteristics may exist between an air-inflated membrane and a water-inflated membrane. Therefore, in Chapter 2, some aspects of the free vibrations of an air-inflated cylindrical membrane are presented, which are similar to Firt's work [4]. Some typical

mode shapes are plotted, and the relationship between the eigenvalues and the central angle of the membrane curve is obtained.

The equilibrium analysis of a water-filled membrane under hydrostatic conditions is presented in Chapter 3, in which the boundary value problem of the static profile is formulated and solved.

The obtained equilibrium shape is then used in Chapter 4, in the derivation of the equation of motion of the water-inflated membrane. Only the case with no water outside the membrane is considered in this chapter. The hydrodynamic pressures are expressed in terms of the membrane displacement vectors, with the use of a boundary element method and Bernoulli's equation. Thus the eigenvalue problem is formulated, and then solved by applying a finite difference method. The computed natural frequencies are compared to some experimental results.

In Chapter 5, the analysis is extended to include the hydrodynamic effect from an upstream head. The surface wave effect is assumed to be small, and the boundary element method is again applied.

Chapter 6 presents a summary of this investigation and some future research suggestions.

1.2 Literature Review

The shape of an inflatable membrane dam under static loading was investigated in many papers. Anwar [5] presented a theory to find the static profiles of a water-inflated dam, as well as an air-inflated dam when the impounding water was at the crest. Binnie [6] derived a closed form solution under the same static condition, but concentrated on a water-inflated dam, and Irvine [7] performed a similar analysis. The base width and perimeter length were taken into account, and the relations between these factors, the internal pressure, and the dam height were obtained.

Harrison [8] developed a finite element technique, while Parbery [9] used a continuous method including a Newton-Raphson scheme to solve the differential equations of equilibrium for air-inflated and water-inflated membrane dams; the effects of the variations of some parameters were presented in figures. The former paper also pointed out that there were significant differences in the analysis of the inflatable membrane from that of a loaded cable. Since the solution of the equilib-

rium equations might not be unique, the latter paper suggested that the upstream head, instead of the upstream membrane angle, and the membrane tension be the two unknowns to be determined. Furthermore, this method was modified, such that it could deal with the loading conditions under which the membrane near the downstream end was laid flat. With this treatment, difficulties encountered in the static analysis of a nearly full membrane dam were overcome. These numerical methods are very general, and can be easily applied in practical cases.

An air-inflated membrane dam was considered by Parbery [10], and the effects of perimeter length, membrane weight and elasticity were examined numerically. Assuming the membrane to be weightless, a theoretical solution was derived, and was applicable for any level of retained water head. Hitch and Narayanan [11] presented figures showing the relations between the parameters of the equilibrium equations of a water-inflated dam when the retained water was at the crest. Watson [12] analyzed the shape of a water-filled or an air-filled dam theoretically, when the water was at the crest. In particular, he presented results which might be useful in the design of these dams.

A comprehensive study on the statics and the dynamics of an air-inflated membrane was reported in Firt [4], in which various loading conditions, such as wind loads and snow loads, were considered. Part of his work on the free vibrations of cylindrical membranes is discussed in Chapter 2. Fagan [13] reported that the effect of membrane weight on the free vibrational response of an air-inflated membrane, which was weightless and impounded no water, was minor. Nonlinear vibrations were considered by Leeuwrik [14], and analyzed using a Galerkin approximation method.

Two series of model experiments were carried out by Baker, Buxton and Worster [15] to investigate the vibrations and stability of the flexible water-inflated membrane for the Mangla Dam Project in Pakistan, under overflow conditions. They observed that the sectional model would vibrate and fluctuations in tension would become larger when increasing the head of the overflow. However, the effects of the end conditions and the damping factor could not be determined. It was indicated that natural ventilation was the most effective method in lowering vibrations.

DAM	LOCATION	HEIGHT (FT)	LENGTH (FT)	FUNCTION	INSTALLED
ALAMEDA CREEK #1	FREMONT, CA	13.0	210.0	WATER DIVERSION	1972
ALAMEDA CREEK #2	FREMONT, CA	6.2	170.0	WATER DIVERSION	1975
ARCHUSA CREEK #1,2	HATTIESBURG, MS	5.0	55.0	RECREATION	1971
ARVIN EDISON	ARVIN, CA	2.3	110.0	FLOW DIVERSION FOR POWER FAILURE	1966
AUSTRIAN DAM	SAN JOSE, CA	2.0	62.0	INCREASE RESERVOIR CAPACITY	1959
BEARDSLEY INTAKE	SAN JOSE, CA	1.0	20.0	INCREASE INTAKE EFFICIENCY	1970
CELERYVILLE DAMS #1,2	HILLIARD, OH	8.0	30.0	STORAGE, IRRIGATION, FLOOD CONTROL	1965
CELERYVILLE DAM #3	HILLIARD, OH	8.0	4.0	STORAGE, IRRIGATION, FLOOD CONTROL	1965
CELERYVILLE DAM #4	HILLIARD, OH	7.0	4.0	STORAGE, IRRIGATION, FLOOD CONTROL	1965
CONGRESS SPRINGS	SAN JOSE, CA	2.0	32.0	WATER DIVERSION	1961
COORS FABRIDAM	GOLDEN, CO	5.0	60.0	WATER POOL FOR PLANT COOLING	1977
CRAIGS POND	DOVER, DE	5.0	10.0	RECREATION, FISH, WILDLIFE DEVELOPMENT	1964
DISNEYWORLD DAM	LAKE BUENO VISTA, FL	6.0	140.0	MAINTAIN COVE WATER LEVEL	1976
FELTON DAM	SANTA CRUZ, CA	8.0	75.0	POOL FOR PUMPING STATION	1975
FLINT RIVER #1, 2	FLINT, MI	6.0	56.0	FLOOD CONTROL CHANNEL IMPROVEMENT	1978
GUADALUPE DAMS #1, 2	SEQUIN, TX	10.0	50.0	BARRIER FOR TIDAL AND SALINITY CONTROL	1965
HIRSHFIELD BROOK DAM	ORADELL, NJ	3.3	24.0	INCREASE WATER STORAGE	1966
HOFFMAN-LA ROCHE DAMS #1, 2	BELVEDERE, NJ	(4.0-FT DIAMETER)		BLOCK DRAINAGE AND LOWER SPILLAGE	1973
HOLIDAY CAMPLANDS	ANDOVER, OH	5.0	30.0	RECREATION	1975
KOOMBOOLOOMBA DAM	TULLY FALLS, AUSTRALIA	5.0	200.0	INCREASE DAM STORAGE	1967
LAKE ALTOONA	ALTOONA, PA	4.0	124.0	INCREASE CITY WATER SUPPLY STORAGE	1969
LOS ANGELES RIVER	LOS ANGELES, CA	5.0	125.0	UNDERGROUND STORAGE WATER DIVERSION	1959
LOWER CAHANEE INTAKE	SAN JOSE, CA	4.0	21.0	INCREASE HEAD ON INTAKE	1963
MANGLA SPILLWAY CONTROL DAMS	MANGLA, PAKISTAN	10.0	225.0	REGULATE TUNNEL SURGE AND TAILWATER	1971
MAPLE GROVE RESERVOIR #1	DENVER, CO	6.0	30.0	INCREASE SPILLWAY CAPACITY	1977
MAPLE GROVE RESERVOIR #2	DENVER, CO	10.0	40.0	INCREASE SPILLWAY CAPACITY	1977
MAURICE RIVER (UNION LAKE)	HAWA, PA	2.5	117.0	INCREASE AND MAINTAIN LAKE LEVEL	1965
MILL RUN RESERVOIR	ALTOONA, PA	4.0	50.0	INCREASE STORAGE CAPACITY	1968
MITCHELL CREEK	FLORENCE, SC	8.0	19.0	IRRIGATION AND FLOOD CONTROL	1981
MOUNT STERLING DAM #1	MOUNT STERLING, KY	3.0	100.0	INCREASE RESERVOIR STORAGE CAPACITY	1966
MOUNT STERLING DAM #2	MOUNT STERLING, KY	2.0	37.0	INCREASE RESERVOIR STORAGE CAPACITY	1966
NEBRASKA CITY POWER ST. #1-6	NEBRASKA CITY, NE	6.0	12.0	RESTRAIN MUD	1978
OSTHALD INTAKE DAM	SAN JOSE, CA	10.0	120.0	INCREASE INTAKE HEAD	1961
PLATTE RIVER CANOE CHUTE DAM	DENVER, CO	3.0	5.0	RECREATION	1976
PRUSTON HEIR DAM	STUART RIVER, AUSTRALIA	5.0	167.0	INCREASE STORAGE CAPACITY	N.A.
RICHLAND CREEK	PULASKI,TN	3.0	119.0	INCREASE LAKE LEVEL	1972
RUFE HYSONG DAM #1	BROOKSVILLE, FL	5.0	250.0	RECREATION, BOAT LOCKS	1965
RUFE HYSONG DAM #2, 3	BROOKSVILLE, FL	9.0	17.0	RECREATION, BOAT LOCKS	1965
RUSSIAN RIVER	SANTA ROSA, CA	11.0	123.0	UNDERGROUND STORAGE WATER DIVERSION	1975
ST. LOUIS RIVER DAMS #1, 2	EVELETH, MN	10.0	50.0	IRON ORE PROCESSING WATER STORAGE	1964
SAND CREEK DAM	NEWTON, KS	8.0	70.0	RECREATION AND CITY BEAUTIFICATION	1965
SAN GABRIEL RIVER #1, 2	LOS ANGELES, CA	2.0	99.0	UNDERGROUND STORAGE WATER DIVERSION	1968
SUNBURY DAMS #1-6	HARRISBURG, PA	7.8	300.0	RECREATION ALONG SUSQUEHANNA RIVER	1970
SUNBURY DAM #7	HARRISBURG, PA	7.8	175.0	RECREATION ALONG SUSQUEHANNA RIVER	1970
TUCOMBIL ESCAPE CONTROL DAM	RICHMOND RIVER, AUSTRALIA	6.0	200.0	CHECK VALVE AND SALINITY BARRIER	N.A.
TUJUNGA CREEK	LOS ANGELES, CA	6.0	197.0	UNDERGROUND STORAGE WATER DIVERSION	1965
WAIALUA DAM	WAIALUA, HW	6.0	197.0	INCREASE AGRICULTURAL STORAGE CAPACITY	1969
ZUNI DAM	DENVER, CO	6.0	150.0	POOL FOR PLANT COOLING WATER	1974

Table 1.1 Features of Some Inflatable Dams in the United States
(Adapted largely from the information brochure, "Imbertson Fabridam," N.M. Imbertson & Associates, Inc., 2213 W. Burbank Blvd., Burbank, CA)

Chapter 2

FREE VIBRATIONS OF AIR-INFLATED MEMBRANE

This chapter deals with the free vibrations of an air-inflated membrane, in the absence of any external pressure. It is expected that similar vibrational modes may exist in the dynamic response of a water-inflated membrane. Firt's book [4] has treated this topic, and here we discuss it in a similar manner. In addition, mode shapes and the relationship of the eigenvalues to the central angle of the membrane curve are presented in figures.

It is observed that the static membrane shape is circular, due to the constant pressure difference. Results are based on the assumptions that the displacements of the membrane are small and its extension, as well as the effect of damping, are negligible during vibrations.

2.1 Equation of Motion

Let us consider a membrane element of length dS in the dynamic state shown in Fig. 2.1. The tangential and radial displacements at any point θ and time t are denoted by $v(\theta,t)$ and $w(\theta,t)$, respectively. The membrane tension T is also a function of both θ and t. The mass per unit length is denoted by μ.

The equation of motion in the tangential direction has the form

$$\mu dS \frac{\partial^2 v}{\partial t^2} = -T + (T + \frac{\partial T}{\partial \theta} d\theta) \cos d\theta + q dS \sin \frac{d\theta}{2}. \tag{2.1}$$

The equation of motion in the radial direction yields

$$\mu dS \frac{\partial^2 w}{\partial t^2} = T \sin \frac{d\theta}{2} + (T + \frac{\partial T}{\partial \theta} d\theta) \sin \frac{d\theta}{2} - q dS. \tag{2.2}$$

Considering small vibrations, we have

$$\cos d\theta \cong 1, \quad \sin d\theta \cong d\theta, \quad \sin \frac{d\theta}{2} \cong \frac{d\theta}{2}. \tag{2.3}$$

Ignoring the second and higher power terms involving dS and $d\theta$, and cancelling appropriate terms, equations (2.1)-(2.2) are reduced to

$$\mu \frac{\partial^2 v}{\partial t^2} = \frac{\partial T}{\partial \theta} \frac{\partial \theta}{\partial S}, \tag{2.4}$$

$$\mu \frac{\partial^2 w}{\partial t^2} = T \frac{\partial \theta}{\partial S} - q. \tag{2.5}$$

The geometric relationship between the curvature of the dynamic state, $\partial\theta/\partial S$, and that of the equilibrium state, $d\theta_0/dS$, is also used in the derivation of the dynamic equation. From Henrych [16], we recall

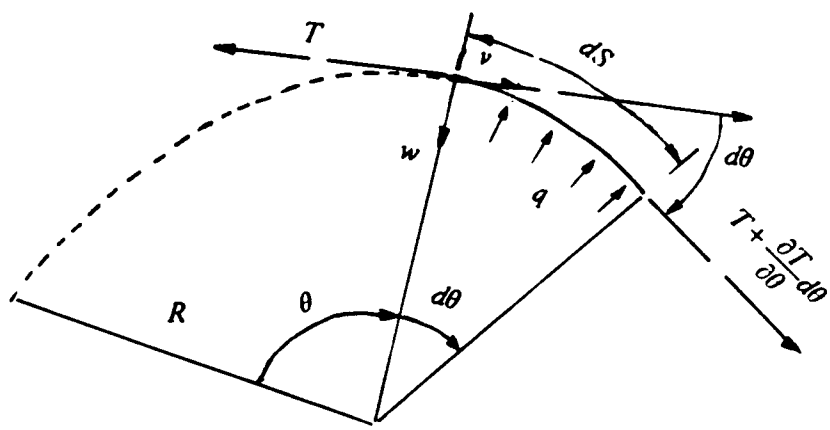

Fig. 2.1 Forces on Element of Air-Inflated Membrane

$$\frac{\partial\theta}{\partial S}=\frac{1}{R}+\frac{1}{K}\left[\frac{1}{R^2}\frac{\partial^2 w}{\partial\theta^2}+\frac{w}{R^2}+\frac{d}{dS}\left(\frac{1}{R}\right)v\right] \tag{2.6}$$

where

$$K=1+\frac{\partial w}{\partial S}-\frac{1}{R}w \quad \text{and} \quad \frac{1}{R}=\frac{d\theta_0}{dS}. \tag{2.7}$$

Since R is constant for the circular air-inflated membrane, we note that the last term in the brackets of equation (2.6) vanishes. Considering small dynamic deflections($K=1$), equation (2.6) leads to

$$\frac{\partial\theta}{\partial S}=\frac{1}{R}\left[1+\frac{1}{R}\frac{\partial^2 w}{\partial\theta^2}+\frac{w}{R}\right]. \tag{2.8}$$

Substituting equation (2.8) into (2.4) and (2.5), we get

$$\mu\frac{\partial^2 v}{\partial t^2}=\frac{\partial T}{\partial\theta}\left(\frac{1}{R}+\frac{1}{R^2}\frac{\partial^2 w}{\partial\theta^2}+\frac{w}{R^2}\right), \tag{2.9}$$

$$\mu\frac{\partial^2 w}{\partial t^2}=T\left(\frac{1}{R}+\frac{1}{R^2}\frac{\partial^2 w}{\partial\theta^2}+\frac{w}{R^2}\right)-q. \tag{2.10}$$

It is observed that T can be removed by combining equations (2.9)-(2.10) into one equation of motion. Solving equation (2.10) for T yields

$$T=\left(\frac{1}{R}+\frac{1}{R^2}\frac{\partial^2 w}{\partial\theta^2}+\frac{w}{R^2}\right)^{-1}\left(\mu\frac{\partial^2 w}{\partial t^2}+q\right). \tag{2.11}$$

Differentiating this with respect to θ and noting that both q and R are constant, we obtain

$$\frac{\partial T}{\partial\theta}=-\left(\frac{1}{R}+\frac{1}{R^2}\frac{\partial^2 w}{\partial\theta^2}+\frac{w}{R^2}\right)^{-2}\left(\frac{1}{R^2}\frac{\partial^3 w}{\partial\theta^3}+\frac{1}{R^2}\frac{\partial w}{\partial\theta}\right)\left(\mu\frac{\partial^2 w}{\partial t^2}+q\right)$$
$$+\left(\frac{1}{R}+\frac{1}{R^2}\frac{\partial^2 w}{\partial\theta^2}+\frac{w}{R^2}\right)^{-1}\left(\mu\frac{\partial^3 w}{\partial\theta\partial t^2}\right).$$

Inserting this into equation (2.9), we have

$$\mu\frac{\partial^2 v}{\partial t^2} = -\left(\frac{1}{R}+\frac{1}{R^2}\,\frac{\partial^2 w}{\partial\theta^2}+\frac{w}{R^2}\right)^{-1}\left(\frac{1}{R^2}\,\frac{\partial^3 w}{\partial\theta^3}+\frac{1}{R^2}\,\frac{\partial w}{\partial\theta}\right)\left(\mu\frac{\partial^2 w}{\partial t^2}+q\right) + \mu\frac{\partial^3 w}{\partial\theta\partial t^2}. \tag{2.12}$$

Carrying out the linearization of the above equation, we have

$$\mu\frac{\partial^2 v}{\partial t^2} = -\frac{q}{R}\left(\frac{\partial^3 w}{\partial\theta^3}+\frac{\partial w}{\partial\theta}\right)+\mu\frac{\partial^3 w}{\partial\theta\partial t^2}. \tag{2.13}$$

Furthermore, v and w can be related directly using the previous assumption of membrane inextensibility. Let the original element length and deformed element length be denoted as N and M, respectively, as shown in Fig. 2.2. It follows that

$$N = Rd\theta, \tag{2.14}$$

$$\begin{aligned} M &= (R-w)d\theta+\left(\frac{v+dv}{R}\right)(R-w)-\left(\frac{v}{R}\right)(R-w)\\ &= Rd\theta - wd\theta + dv. \end{aligned} \tag{2.15}$$

We note that the above calculation has assumed small dynamic deflection, such that $(R-w)/R \cong 1$. Let us then denote ε as the membrane strain, which is equal to zero because of inextensibility. We have

$$\varepsilon = 0 = \frac{M-N}{N} = \frac{1}{R}\left(-w+\frac{dv}{d\theta}\right). \tag{2.16}$$

Thus,

$$w = \frac{dv}{d\theta}. \tag{2.17}$$

Therefore, differentiating equation (2.13) with respect to θ and using (2.17), we obtain the equation of motion for the free vibrations of the air-inflated membrane in the radial direction:

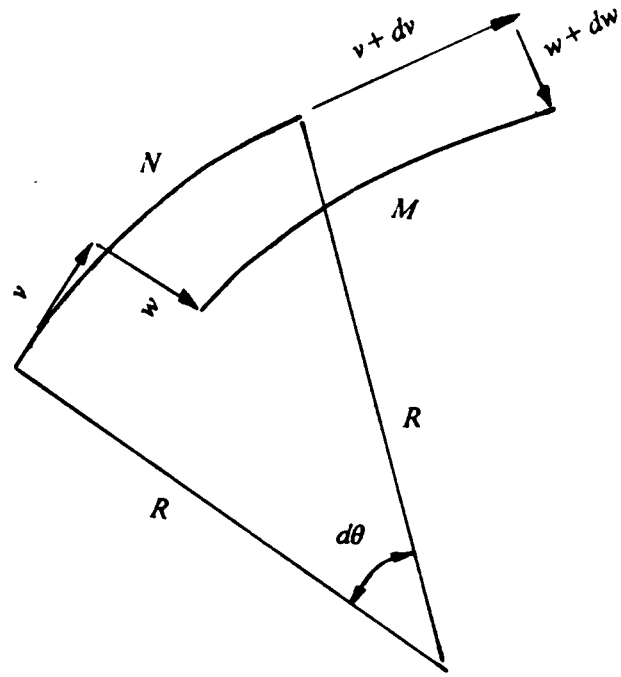

Fig. 2.2 Element of Equilibrium and Dynamic State

$$\frac{\partial^4 w}{\partial \theta^4} + \frac{\partial^2}{\partial \theta^2}\left(w - \frac{\mu R}{q}\frac{\partial^2 w}{\partial t^2}\right) + \frac{\mu R}{q}\frac{\partial^2 w}{\partial t^2} = 0. \tag{2.18}$$

Now, separating w in space and time, we let

$$w(\theta,t) = \hat{w}(\theta)\sin \omega t \tag{2.19}$$

which satisfies equation (2.18). Introducing equation (2.19) into (2.18), it follows that

$$\frac{d^4\hat{w}}{d\theta^4} + (1+\lambda)\frac{d^2\hat{w}}{d\theta^2} - \lambda\hat{w} = 0 \tag{2.20}$$

where

$$\lambda = \frac{\mu\omega^2 R}{q}. \tag{2.21}$$

2.2 Vibration Frequencies and Mode Shapes

Following the work of Firt [4], we substitute $\hat{w} = e^{\beta\theta}$ into equation (2.20) and obtain

$$\beta^4 + (1+\lambda)\beta^2 - \lambda = 0 \tag{2.22}$$

which has roots

$$\begin{aligned} \beta_{1,2} &= \pm\frac{i}{\sqrt{2}}\sqrt{1+\lambda+\sqrt{1+6\lambda+\lambda^2}}, \\ \beta_{3,4} &= \pm\frac{1}{\sqrt{2}}\sqrt{-1-\lambda+\sqrt{1+6\lambda+\lambda^2}}. \end{aligned} \tag{2.23}$$

It follows that we can write the general solution of equation (2.20) in the form

$$\hat{w} = C_1 \sin a\frac{\theta}{\alpha} + C_2 \cos a\frac{\theta}{\alpha} + C_3 \sinh b\frac{\theta}{\alpha} + C_4 \cosh b\frac{\theta}{\alpha} \tag{2.24}$$

where α is the central angle of the circular membrane arc,

$$a = \frac{\alpha}{\sqrt{2}}\sqrt{1 + \lambda + \sqrt{1 + 6\lambda + \lambda^2}}\,, \tag{2.25}$$

$$b = \frac{\alpha}{\sqrt{2}}\sqrt{-1 - \lambda + \sqrt{1 + 6\lambda + \lambda^2}}\,, \tag{2.26}$$

and C_i are constants of integration. Also, from equation (2.17) and by assuming

$$v(\theta,t) = \hat{v}(\theta)\sin \omega t$$

we can write

$$\hat{v} = -C_1\frac{\alpha}{a}\cos a\frac{\theta}{\alpha} + C_2\frac{\alpha}{a}\sin a\frac{\theta}{\alpha} + C_3\frac{\alpha}{b}\cosh b\frac{\theta}{\alpha} + C_4\frac{\alpha}{b}\sinh b\frac{\theta}{\alpha} + C_5\,. \tag{2.27}$$

The integration constant C_5 is caused by the rotation of the circular membrane about its center. The air-inflated membrane as shown in Fig. 2.3 does not allow such rotation during vibrations because both ends are anchored; thus

$$C_5 = 0. \tag{2.28}$$

The boundary conditions are

$$\begin{aligned} &\hat{w}(0) = 0, \quad \hat{v}(0) = 0, \\ &\hat{w}(\alpha) = 0, \quad \hat{v}(\alpha) = 0. \end{aligned} \tag{2.29}$$

Applying these to equations (2.24) and (2.27) leads to the following simultaneous equations:

$$C_2 + C_4 = 0, \tag{2.30}$$

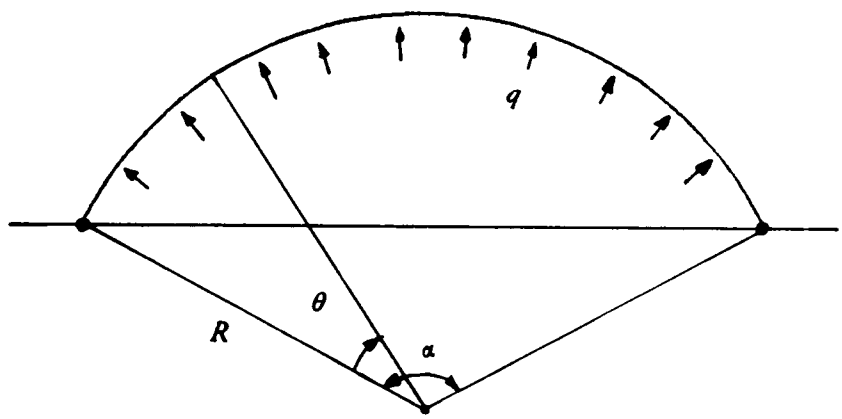

Fig. 2.3 Geometry of an Air-Inflated Membrane

$$C_1 \sin a + C_2 \cos a + C_3 \sinh b + C_4 \cosh b = 0, \tag{2.31}$$

$$-C_1 \frac{1}{a} + C_3 \frac{1}{b} = 0, \tag{2.32}$$

$$-C_1 \frac{1}{a} \cos a + C_2 \frac{1}{a} \sin a + C_3 \frac{1}{b} \cosh b + C_4 \frac{1}{b} \sinh b = 0. \tag{2.33}$$

For a nontrivial solution to exist, we can put equations (2.30)-(2.33) in matrix form and then set the determinant equal to zero:

$$\begin{vmatrix} 0 & 1 & 0 & 1 \\ \sin a & \cos a & \sinh b & \cosh b \\ -\frac{1}{a} & 0 & \frac{1}{b} & 0 \\ -\frac{\cos a}{a} & \frac{\sin a}{a} & \frac{\cosh b}{b} & \frac{\sinh b}{b} \end{vmatrix} = 0. \tag{2.34}$$

After simplification, we obtain the characteristic equation

$$2(1 - \cos a \cosh b) + \frac{b^2 - a^2}{ab} \sin a \sinh b = 0. \tag{2.35}$$

The solution of the characteristic equation can be found by using a root-finding subroutine. The lowest four eigenvalues (λ_i, $i = 1,2,3,4$) corresponding to a series of α, ranging from 0.754 to 2π, are calculated and shown in Table 2.1 and Fig. 2.4. Firt has obtained the first four frequencies for $\alpha = \pi$ as

$$\lambda_1 = 1.71, \quad \lambda_2 = 5.97, \quad \lambda_3 = 13.07, \quad \lambda_4 = 21.86,$$

which are slightly higher than the values at $\alpha = \pi$ shown in Table 2.1. It is observed that the natural vibration frequencies increase rapidly when α decreases below π.

The mode shapes can be found by solving the three boundary equations (2.30)-(2.32) to get C_2, C_3, and C_4 in terms of C_1 , and the result is inserted into equations (2.24) and (2.27) to yield

$20\alpha/\pi$	λ_1	λ_2	λ_3	λ_4
2	396.0289	815.6384	1596.0200	2416.0565
3	173.8420	361.0340	707.1545	1072.3259
4	96.1128	201.9293	396.0757	602.0235
5	60.1736	128.2941	252.1158	384.3442
6	40.6901	88.3025	173.9406	266.1024
7	28.9805	64.1968	126.8280	194.8101
8	21.4178	48.5595	96.2734	148.5426
9	16.2683	37.8467	75.3472	116.8256
10	12.6182	30.1920	60.3992	94.1425
11	9.9486	24.5364	49.3579	77.3634
12	7.9468	20.2428	40.9770	64.6054
13	6.4151	16.9090	34.4702	54.6803
14	5.2235	14.2713	29.3210	46.8088
15	4.2836	12.1507	25.1795	40.4620
16	3.5335	10.4222	21.8012	35.2712
17	2.9290	8.9965	19.0115	30.9725
18	2.4377	7.8084	16.6829	27.3735
19	2.0355	6.8092	14.7205	24.3309
20	1.7040	5.9622	13.0526	21.7363
21	1.4293	5.2391	11.6241	19.5065
22	1.2005	4.6179	10.3922	17.5768
23	1.0091	4.0813	9.3231	15.8960
24	0.8483	3.6153	8.3902	14.4238
25	0.7128	3.2089	7.5718	13.1272
26	0.5981	2.8530	6.8506	11.9800
27	0.5008	2.5401	6.2122	10.9604
28	0.4181	2.2642	5.6449	10.0504
29	0.3475	2.0202	5.1390	9.2353
30	0.2872	1.8037	4.6862	8.5026
31	0.2356	1.6112	4.2798	7.8418
32	0.1913	1.4397	3.9139	7.2440
33	0.1533	1.2864	3.5837	6.7019
34	0.1206	1.1493	3.2849	6.2088
35	0.0924	1.0264	3.0139	5.7592
36	0.0681	0.9161	2.7676	5.3485
37	0.0471	0.8168	2.5433	4.9723
38	0.0291	0.7275	2.3388	4.6272
39	0.0135	0.6469	2.1518	4.3099
40	0.0000	0.5742	1.9807	4.0178

Table 2.1 The First Four λ Values vs. α

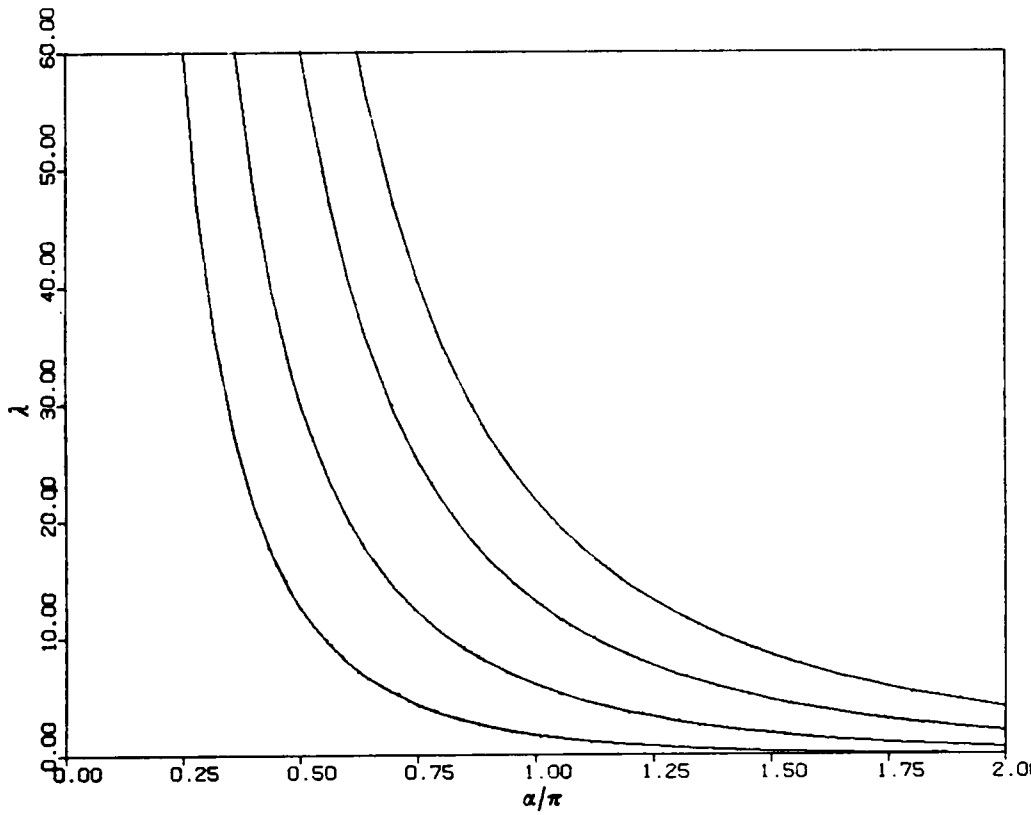

Fig. 2.4 The First Four Eigenvalues λ vs. α/π

$$\hat{w} = C_1\Big(\sin a\frac{\theta}{\alpha} + H\cos a\frac{\theta}{\alpha} + \frac{b}{a}\sinh b\frac{\theta}{\alpha} - H\cosh b\frac{\theta}{\alpha} \Big), \tag{2.36}$$

$$\hat{v} = C_1\frac{\alpha}{a}\Big(-\cos a\frac{\theta}{\alpha} + H\sin a\frac{\dot{\theta}}{\alpha} + \cosh b\frac{\theta}{\alpha} - H\frac{a}{b}\sinh b\frac{\theta}{\alpha} \Big), \tag{2.37}$$

where

$$H = -\frac{\sin a + \frac{b}{a}\sinh b}{\cos a - \cosh b}. \tag{2.38}$$

The first four mode shapes are plotted in Fig. 2.5 for $\alpha = \pi$. We note that the lowest mode is anti-symmetric, and is different from the first mode of free vibrations of a pinned-pinned beam, which is symmetric and of a single sign (i.e., has no node). This is understandable because the membrane here is inextensible, and this symmetric mode is invalid. We note that the integral of $\hat{w}$ over the membrane curve is equal to zero, i.e., using equations (2.17) and (2.19),

$$\int_0^\alpha \hat{w}(\theta)d\theta = \hat{v}(\alpha) - \hat{v}(0) = 0. \tag{2.39}$$

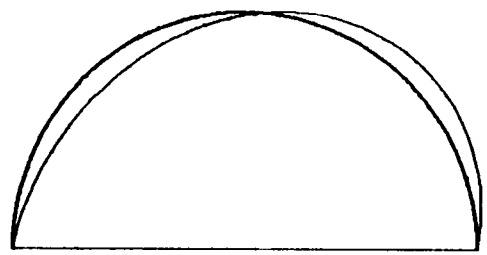

(a) $\lambda_1 = 1.704$

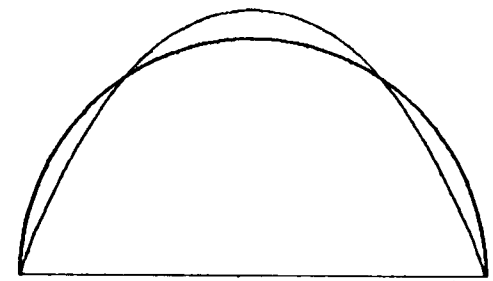

(b) $\lambda_2 = 5.962$

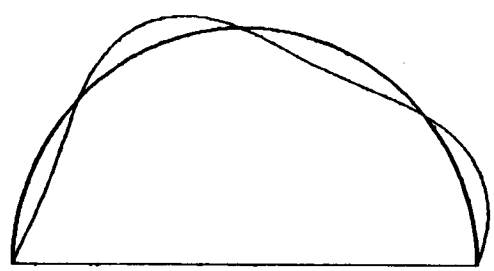

(c) $\lambda_3 = 13.053$

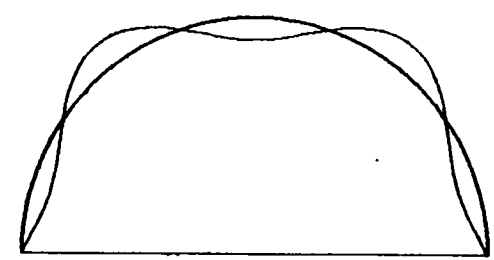

(d) $\lambda_4 = 21.736$

Fig. 2.5 Mode Shapes for $\alpha = \pi$

Chapter 3

STATIC ANALYSIS

In this chapter, the equilibrium analysis of the shape of the water-inflated membrane dam under static water forces is presented. The membrane may have a water head on the upstream dam face as illustrated in Fig. 3.1. Employing a Runge-Kutta procedure for the integration of the differential equations, along with an iterative scheme, the static profile is found. The obtained equilibrium shape and tension are used in the derivation of the equation of motion of the membrane in the next chapter.

The membrane weight is neglected, since there are usually much higher pressures on the membrane from the internal water head. In addition, it is assumed that the membrane material is inextensible. Parbery [10] has justified that the influences of the membrane weight and elasticity on the static shape and tension are minor and negligible. For a treatment which includes both the membrane weight and elasticity, the reader is referred to Harrison [8] and Parbery [9].

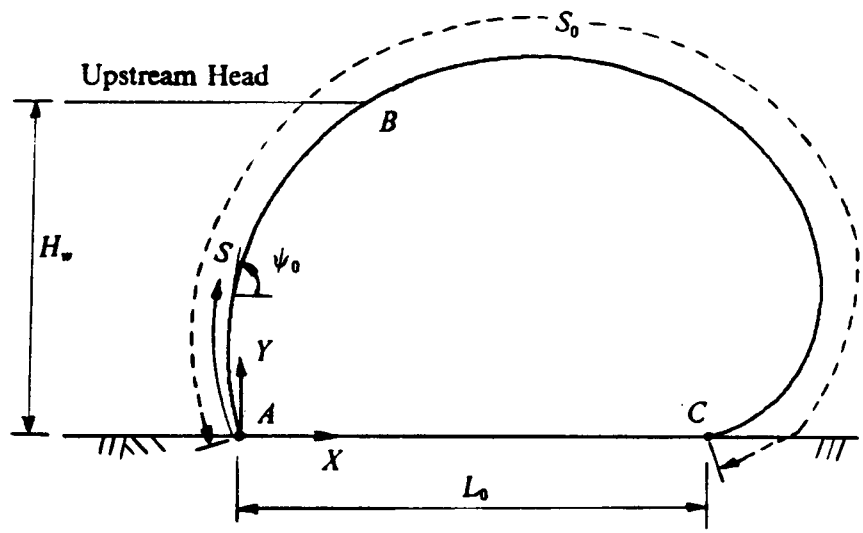

Fig. 3.1 Cross-Section of a Water-Inflated Membrane with Upstream Head

3.1 Equation of Equilibrium

Let us consider a differential element dS of unit width, where S is the arc length and S_0 is the perimeter. The loading condition is shown in Fig. 3.2, where T_0 is the tension per unit width, q is the net normal pressure and ψ_0 is the angle of the membrane measured counter-clockwise from the X coordinate.

Summing forces in the tangential direction gives

$$-T_0+\left[T_0+\left(\frac{dT_0}{dS}\right)dS\right]\cos d\psi_0=0. \tag{3.1}$$

Similarly, summing forces in the radial direction gives

$$\left[T_0+\left(\frac{dT_0}{dS}\right)dS\right]\sin d\psi_0+qdS=0. \tag{3.2}$$

It is assumed that $d\psi_0$ is small such that

$$\cos d\psi_0 \cong 1, \qquad \sin d\psi_0 \cong d\psi_0.$$

Therefore, after neglecting products of ds and $d\psi_0$, and cancelling proper terms, equations (3.1)-(3.2) lead to

$$\frac{dT_0}{dS}=0, \tag{3.3}$$

$$\frac{d\psi_0}{dS}=-\frac{q}{T_0}, \tag{3.4}$$

in which equation (3.3) implies that T_0 is a constant along the perimeter.

Geometrically, we have

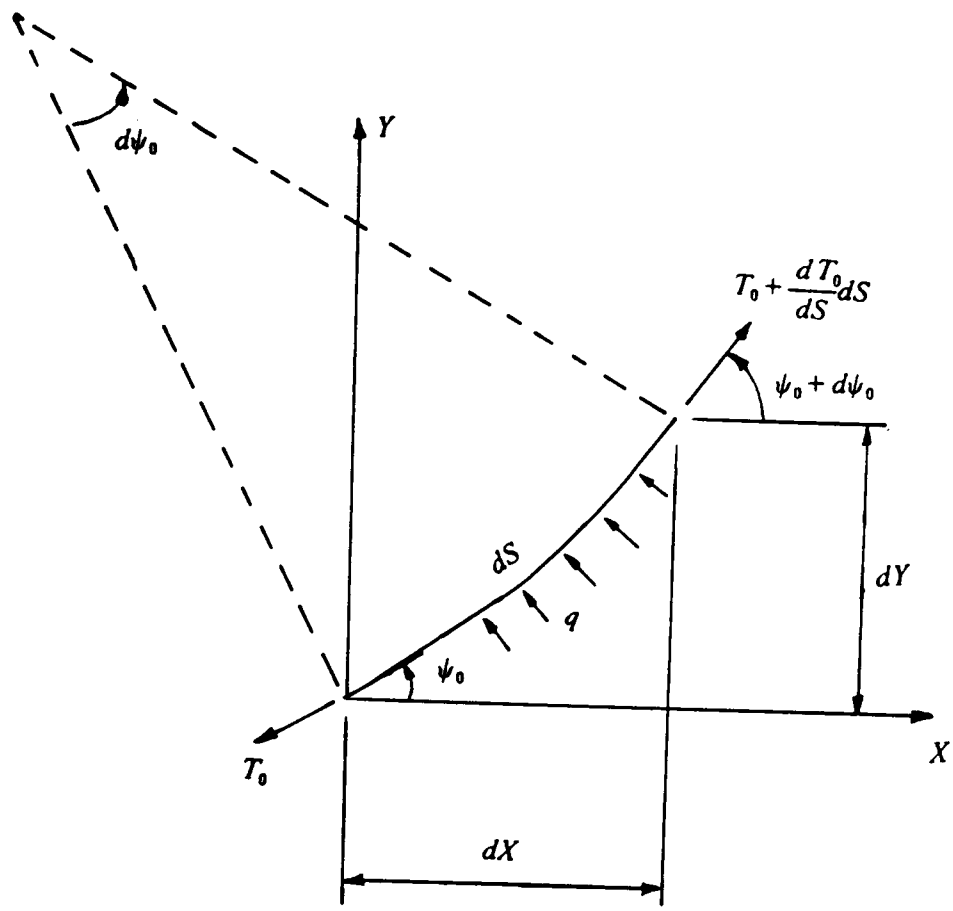

Fig. 3.2 Static Equilibrium of an Element

$$\frac{dX}{dS} = \cos\psi_0, \tag{3.5}$$

$$\frac{dY}{dS} = \sin\psi_0. \tag{3.6}$$

We note that, in Fig. 3.1,

$$q = \gamma(H_i - H_w) \qquad \text{from A to B,} \tag{3.7a}$$

$$q = \gamma(H_i - Y) \qquad \text{from B to C,} \tag{3.7b}$$

which come from the hydrostatic forces, where γ is the specific weight of water, H_i is the internal head and H_w is the upstream head.

It is convenient to introduce the following non-dimensional variables:

$$x = \frac{X}{L_0}, \quad y = \frac{Y}{L_0}, \quad s = \frac{S}{L_0}, \quad s_0 = \frac{S_0}{L_0}, \quad h_i = \frac{H_i}{L_0}, \quad h_w = \frac{H_w}{L_0}, \tag{3.8}$$

where L_0 is the base length.

To find the non-dimensional tension t_0, let us write

$$T_0 = \ell t_0$$

where ℓ is an unknown dimensional factor. Introducing this into equation (3.4) and using the relationships in equation (3.7) for q , it is easy to find that

$$\ell = \gamma L_0^2$$

which leads to

$$t_0 = \frac{T_0}{\gamma L_0^2}. \tag{3.9}$$

Making use of the non-dimensional parameters and equation (3.7), equations (3.4)-(3.6) become

$$\frac{d\psi_0}{ds} = \frac{(h_w - h_i)}{t_0} \qquad \text{from A to B,} \tag{3.10a}$$

$$\frac{d\psi_0}{ds} = \frac{(y - h_i)}{t_0} \qquad \text{from B to C,} \tag{3.10b}$$

$$\frac{dx}{ds} = \cos\psi_0, \tag{3.11}$$

$$\frac{dy}{ds} = \sin\psi_0. \tag{3.12}$$

The differential equations (3.10)-(3.12), together with the boundary conditions

$$x(0) = 0, \tag{3.13}$$

$$y(0) = 0, \tag{3.14}$$

$$x(s_0) = 1, \tag{3.15}$$

$$y(s_0) = 0, \tag{3.16}$$

which come from the ends of the membrane cross section, form the two-point boundary value problem of the membrane. We note that the non-dimensional base length is equal to 1, as stated in equation (3.15).

The upstream face has a portion of circular shape due to the constant pressure difference and constant membrane tension, provided that there is an upstream head, as shown in Fig. 3.1. Equation (3.10) can be easily modified for loading conditions having no water on the upstream face, or conditions involving a tail water. In the cases of no water outside the membrane, we use the second formula of equation (3.10) through the whole membrane curve, while for the cases having a downstream head, another formula must be inserted into equation (3.10) to account for the water pressure changes on the downstream face.

3.2 Numerical Analysis

For a given inflation condition, the boundary value problem consists of determining the unknown initial condition, $\psi_0(0)$, and the induced membrane tension, t_0, such that the boundary conditions are satisfied. A closed form solution is impossible to obtain, and an iterative shooting method is employed here to solve the nonlinear system of equations. The computation of t_0 comprises the main difficulty in this analysis, since this unknown value is not involved in a boundary condition.

The convergence of the iterative scheme developed by Harrison [8] can easily fail, because of its critical dependence on the closeness of the initial guesses of $\phi_0(0)$ and t_0 to the exact solution. Parbery's scheme [9], which is based on determining h_i and t_0, can not be applied, because the incoherence of h_i with the node on the membrane where h_i is located causes a difficulty for the representation of the hydrodynamic pressure from the upstream head on that node in Chapter 5.

Our method starts by guessing a value for $\psi_0(0)$, evaluating t_0 by the subroutine ZEROIN [17], and modifying t_0 until equation (3.15) is satisfied. We keep on trying different values for $\psi_0(0)$ until we find an interval for $\psi_0(0)$ on which $y(s_0)$ changes sign. Using the method of bisection, the interval then can be used to improve the estimation of $\psi_0(0)$ until the other boundary condition, equation (3.16), is also satisfied. A Runge-Kutta subroutine, DVERK, from the International Mathematics and Statistical Library (IMSL), is used for the numerical integration. It is noted that a proper range of t_0 is required in using ZEROIN, such that the obtained shape is practical and equation (3.15) is satisfied. Applying the above iterative scheme developed here, the difficulty pertaining to the uniqueness of the solution [9] of the differential equations is avoided.

Chapter 4

FREE VIBRATIONS OF WATER-INFLATED MEMBRANE

The linear free vibrations of the water-inflated membrane are investigated here. Using a boundary element method and Bernoulli's equation, the hydrodynamic pressures can be expressed in terms of the displacement vectors along the membrane curve. The finite difference method is employed to obtain the displacement derivatives and hydrodynamic pressure derivatives, and then the eigenvalue problem is formulated.

We follow the static analysis of the previous chapter in deriving the equation of motion. The same definitions of parameters are used.

The water-inflated membrane considered impounds no water outside the membrane. The membrane mass is included in the derivation of the equation of motion, and its effect on the free vibration frequencies is discussed. However, the elasticity of the membrane material is still neglected.

The major difficulty in solving the equation of motion pertains to the calculation of the unknown hydrodynamic pressures on the membrane. We note that through Bernoulli's equation, the

hydrodynamic pressures and the velocity potential are related. So it becomes a potential problem with specified boundary conditions. Also, since the water is assumed to be incompressible and inviscid, its motion can be represented by the two-dimensional Laplace's equation. Applying the boundary element method to the Laplace's equation, the relationship between the hydrodynamic pressures and the membrane displacements is established.

The boundary element method could be replaced by the finite element method in treating the potential problem at hand. The advantages of choosing the former method are that it requires less data preparation effort and takes less time in computation for the same accuracy. In fact, it contracts the dimensions of the problem by one, and we need to produce information on the membrane only. For a description of this method, we refer to Brebbia [18] and Banerjee and Butterfield [19].

A Fortran IV computer program, based on the finite difference and the boundary element methods, is written to solve the eigenvalue problem. A linear approximation for each boundary element is used. The effects of the various parameters of the membrane and the relative density of the membrane and the water are examined.

4.1 Equation of Motion

Again, let us take an infinitesimal membrane element dS of unit width. The positive directions of the tangential displacement v, the radial displacement w, and working forces are shown in Fig. 4.1. The hydrodynamic pressure p acts in the normal direction only. The displacements v and w are assumed to be small.

There are two equations of motion associated with two perpendicular directions of motion. Tangentially, we have

$$\mu dS \frac{\partial^2 v}{\partial t^2} = \left(T_0 + T + \frac{\partial T}{\partial S} dS\right) \cos d\psi - (T_0 + T). \tag{4.1}$$

Radially, the equation of motion is

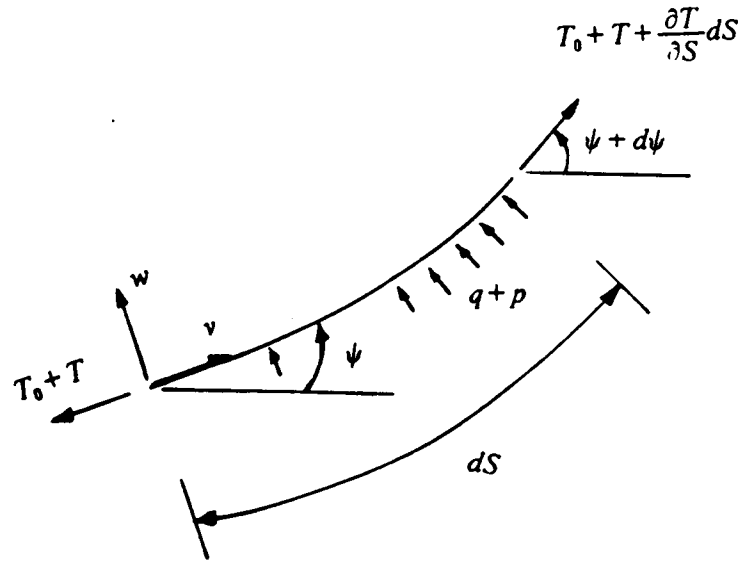

Fig. 4.1 An Element under Dynamic Loading

$$\mu dS \frac{\partial^2 w}{\partial t^2} = \left(T_0 + T + \frac{\partial T}{\partial S} dS\right) \sin \frac{d\psi}{2} + (T_0 + T) \sin \frac{d\psi}{2} + (q + p) dS. \tag{4.2}$$

It is noted that v, w, ψ, p, and T are functions of space S and time t, while q is a function of S only and T_0 is a constant. Since $d\psi$ is small, we can let

$$\cos d\psi \cong 1, \qquad \sin d\psi \cong d\psi, \qquad \sin \frac{d\psi}{2} \cong \frac{d\psi}{2}.$$

Neglecting higher power terms involving dS and $d\psi$, equations (4.1)-(4.2) can be written as

$$\mu \frac{\partial^2 v}{\partial t^2} = \frac{\partial T}{\partial S}, \tag{4.3}$$

$$\mu \frac{\partial^2 w}{\partial t^2} = T_0 \frac{\partial \psi}{\partial S} + T \frac{\partial \psi}{\partial S} + q + p. \tag{4.4}$$

Equations (4.3)-(4.4) can be united into one equation of motion by the elimination of T. Solving equation (4.4) for T gives

$$T = \left(\frac{\partial \psi}{\partial S}\right)^{-1} \left[\mu \frac{\partial^2 w}{\partial t^2} - (q + p)\right] - T_0.$$

Differentiating with respect to S, we obtain

$$\frac{\partial T}{\partial S} = -\left(\frac{\partial \psi}{\partial S}\right)^{-2} \left(\frac{\partial^2 \psi}{\partial S^2}\right) \left[\mu \frac{\partial^2 w}{\partial t^2} - (q + p)\right] + \left(\frac{\partial \psi}{\partial S}\right)^{-1} \left[\mu \frac{\partial^3 w}{\partial S \partial t^2} - \left(\frac{\partial p}{\partial S} + \frac{\partial q}{\partial S}\right)\right].$$

Inserting the above equation into (4.3) and multiplying both sides by $(\partial \psi / \partial S)^2$, we arrive at

$$\mu\left(\frac{\partial\psi}{\partial S}\right)^2\frac{\partial^2 v}{\partial t^2}=-\mu\frac{\partial^2\psi}{\partial S^2}\frac{\partial^2 w}{\partial t^2}+\mu\frac{\partial\psi}{\partial S}\frac{\partial^3 w}{\partial S\partial t^2}+\frac{\partial^2\psi}{\partial S^2}(q+p)-\frac{\partial\psi}{\partial S}\left(\frac{\partial q}{\partial S}+\frac{\partial p}{\partial S}\right). \tag{4.5}$$

In order to be concise, let us rewrite the above equation of motion in the form

$$\mu(\psi_S)^2 v_{tt}=-\mu\psi_{SS}w_{tt}+\mu\psi_S w_{Stt}+\psi_{SS}(q+p)-\psi_S(q_S+p_S) \tag{4.6}$$

where a subscript S denotes a derivative with respect to S, and a subscript t denotes a derivative with respect to t. This notation is adopted for the rest of the work.

There are two relationships which are useful in putting the above equation into a less complicated form: one is between ψ_S and $(\psi_0)_S$, the other is between w and v. First, recalling equation (2.6), using the terminologies in this chapter and considering linear analysis, we have

$$\psi_S=(\psi_0)_S+w_{SS}+[(\psi_0)_S]^2 w+(\psi_0)_{SS}v \tag{4.7}$$

in which we note that $(\psi_0)_S$ is not a constant for the water-inflated membrane.

Secondly, due to the assumption of membrane inextensibility, we obtain

$$w=\frac{\partial v}{\partial\psi} \tag{4.8}$$

(see equation (2.17)). The derivations of the above relationships are similar to those given in Chapter 2 and are not repeated. Applying the chain rule to equation (4.8), we write

$$w=\frac{\partial v}{\partial S}\frac{\partial S}{\partial\psi}=(\psi_S)^{-1}v_S. \tag{4.9}$$

It should be noted that we have considered the dynamic deflections of the membrane to be small.

Let us introduce the following simple notations for the derivatives of ψ_0 with respect to S:

$$A=(\psi_0)_S,\quad B=(\psi_0)_{SS},\quad C=(\psi_0)_{SSS},\quad D=(\psi_0)_{SSSS}. \tag{4.10}$$

Using this notation, we rewrite equation (4.7) as

$$\psi_S = A + w_{SS} + A^2 w + Bv\,. \tag{4.11}$$

Inserting this into equation (4.9) and neglecting nonlinear terms involving v, w and their derivatives, we get

$$w = A^{-1} v_S\,. \tag{4.12}$$

For successful substitutions of equations (4.10)-(4.11) into (4.6), it is required to calculate

$$w_S = -A^{-2} B v_S + A^{-1} v_{SS}\,,$$

$$w_{SS} = v_S(2A^{-3}B^2 - A^{-2}C) - 2A^{-2} B v_{SS} + A^{-1} v_{SSS}\,,$$

$$w_{SSS} = v_S(-6A^{-4}B^3 + 6A^{-3}BC - A^{-2}D) + v_{SS}(6A^{-3}B^2 - 3A^{-2}C) - 3A^{-2} B v_{SSS} + A^{-1} v_{SSSS}\,,$$

$$w_{tt} = A^{-1} v_{Stt}\,,$$

$$w_{Stt} = -A^{-2} B v_{Stt} + A^{-1} v_{SStt}\,,$$

and accordingly

$$\psi_S = A + Bv + v_S(2A^{-3}B^2 - A^{-2}C + A) - 2A^{-2} B v_{SS} + A^{-1} v_{SSS}, \tag{4.13}$$

$$\psi_{SS} = B + Cv + v_S(-6A^{-4}B^3 + 6A^{-3}BC - A^{-2}D + 2B) + v_{SS}(6A^{-3}B^2 - 3A^{-2}C + A) - 3A^{-2} B v_{SSS} + A^{-1} v_{SSSS}. \tag{4.14}$$

Therefore, considering linear analysis, it follows that

$$\begin{aligned}\mu A^2 v_{tt} + \mu 2A^{-1} B v_{Stt} - \mu v_{SStt} &= Bq + Bp \\ &+ \left[Cv + v_S(-6A^{-4}B^3 + 6A^{-3}BC - A^{-2}D + 2B)\right. \\ &\left. + v_{SS}(6A^{-3}B^2 - 3A^{-2}C + A) - 3A^{-2}Bv_{SSS} + A^{-1}v_{SSSS}\right](q+p) \\ &- Aq_S - Ap_S \\ &- \left[Bv + v_S(2A^{-3}B^2 - A^{-2}C + A) - 2A^{-2}Bv_{SS} + A^{-1}v_{SSS}\right](q_S + p_S).\end{aligned} \tag{4.15}$$

Now, let us suppose that p is of the same order as v, which is small, such that when $(q+p)$ or (q_S+p_S) are multiplied by v or its derivatives we can specify

$$q + p \cong q\,, \tag{4.16}$$

$$q_S + p_S \cong q_S\,. \tag{4.17}$$

Moreover, equation (4.15) can be further simplified by replacing q and q_S in terms of the equilibrium membrane tension T_0. From equation (3.4), we can write

$$q = -AT_0 \tag{4.18}$$

and thus

$$q_S = -BT_0\,. \tag{4.19}$$

Substituting equations (4.18)-(4.19) into (4.15), using (4.16)-(4.17) when $(q+p)$ or (q_S+p_S) is multiplied by v or its derivatives, and collecting similar terms, the equation of motion in the tangential direction is in the form of

$$\begin{aligned}\mu A^2 v_{tt} + \mu 2A^{-1} B v_{Stt} - \mu v_{SStt} &= Bp - Ap_S \\ &+ T_0\left[v(-AC + B^2) + v_S(8A^{-3}B^3 - 7A^{-2}BC + A^{-1}D - AB)\right. \\ &+ v_{SS}(-8A^{-2}B^2 + 3A^{-1}C - A^2) \\ &\left. + v_{SSS}(4A^{-1}B) - v_{SSSS}\right].\end{aligned} \tag{4.20}$$

4.2 Dimensional Analysis

It is desirable to nondimensionalize the parameters in the equation of motion as we have done to the differential equations of equilibrium in Chapter 3. Let us recall that

$$s = \frac{S}{L_0}, \quad t_0 = \frac{T_0}{\gamma L_0^2}, \tag{4.21}$$

where L_0 is the base length and γ is the specific weight of water. It is directly perceived that we can add the following nondimensional parameters:

$$\bar{v} = \frac{v}{L_0}, \quad \bar{v}_s = v_S, \quad \bar{v}_{ss} = L_0 v_{SS}, \quad \bar{v}_{sss} = L_0^2 v_{SSS}, \quad \bar{v}_{ssss} = L_0^3 v_{SSSS}, \tag{4.22}$$

$$\bar{A} = L_0 A, \quad \bar{B} = L_0^2 B, \quad \bar{C} = L_0^3 C, \quad \bar{D} = L_0^4 D. \tag{4.23}$$

To determine the nondimensional transformation of the hydrodynamic pressure p and time t, let us define

$$\begin{aligned} \bar{p} &= \frac{p}{\eta}, \\ \bar{t} &= \frac{t}{\beta}. \end{aligned} \tag{4.24}$$

Hence,

$$p_S = \frac{\eta}{L_0} \bar{p}_s,$$

$$v_{tt} = \frac{L_0}{\beta^2} \bar{v}_{\bar{t}\bar{t}},$$

$$v_{Stt} = \frac{\bar{v}_{s\bar{t}\bar{t}}}{\beta^2},$$

$$v_{SSii} = \frac{\bar{v}_{ss\bar{i}\bar{i}}}{\beta^2 L_0}.$$

Equation (4.20) becomes

$$\begin{aligned}\frac{\beta^{-2}}{L_0}\mu\bar{A}^2\bar{v}_{\bar{i}\bar{i}} + \frac{\beta^{-2}}{L_0}\mu 2\bar{A}^{-1}\bar{B}\bar{v}_{s\bar{i}\bar{i}} - \frac{\beta^{-2}}{L_0}\mu\bar{v}_{ss\bar{i}\bar{i}} &= \frac{\eta}{L_0^2}\bar{B}\bar{p} - \frac{\eta}{L_0^2}\bar{A}\bar{p}_s \\ &+ \frac{\gamma}{L_0}t_0\big[\bar{v}(-\bar{A}\bar{C} + \bar{B}^2) \\ &+ \bar{v}_s(8\bar{A}^{-3}\bar{B}^3 - 7\bar{A}^{-2}\bar{B}\bar{C} + \bar{A}^{-1}\bar{D} - \bar{A}\bar{B}) \\ &+ \bar{v}_{ss}(-8\bar{A}^{-2}\bar{B}^2 + 3\bar{A}^{-1}\bar{C} - \bar{A}^2) + \bar{v}_{sss}(4\bar{A}^{-1}\bar{B}) - \bar{v}_{ssss}\big].\end{aligned} \tag{4.25}$$

We can choose η and β to make the coefficients of $\bar{B}\bar{p}$ and $\bar{A}^2\bar{v}_{\bar{i}\bar{i}}$, respectively, equal to γ/L_0. It follows that

$$\eta = \gamma L_0,$$

$$\beta = \sqrt{\frac{\mu}{\gamma}}.$$

Thus, from equation (4.24), we write

$$\bar{p} = \frac{p}{\gamma L_0}, \tag{4.26}$$

$$\bar{t} = \sqrt{\frac{\gamma}{\mu}}\, t. \tag{4.27}$$

Using the dimensionless quantities, therefore, we rewrite equation (4.20) as

$$\begin{aligned}\bar{A}^2\bar{v}_{\bar{i}\bar{i}} + 2\bar{A}^{-1}\bar{B}\bar{v}_{s\bar{i}\bar{i}} - \bar{v}_{ss\bar{i}\bar{i}} &= \bar{B}\bar{p} - \bar{A}\bar{p}_s \\ &+ t_0\big[\bar{v}(-\bar{A}\bar{C} + \bar{B}^2) + \bar{v}_s(8\bar{A}^{-3}\bar{B}^3 - 7\bar{A}^{-2}\bar{B}\bar{C} + \bar{A}^{-1}\bar{D} - \bar{A}\bar{B}) \\ &+ \bar{v}_{ss}(-8\bar{A}^{-2}\bar{B}^2 + 3\bar{A}^{-1}\bar{C} - \bar{A}^2) + \bar{v}_{sss}(4\bar{A}^{-1}\bar{B}) - \bar{v}_{ssss}\big].\end{aligned} \tag{4.28}$$

Consider a vibration in which the displacement $\bar{v}(s, \bar{t})$ is separable in space s and time $\bar{t}$ such that the solution of equation (4.28) can be written in the form

$$\bar{v}(s,\bar{t}) = V(s)\cos\bar{\omega}\bar{t} \tag{4.29}$$

where $\bar{\omega}$ is the nondimensional natural frequency. It follows that the hydrodynamic pressure is harmonic, i.e.,

$$\bar{p}(s,\bar{t}) = P(s)\cos\bar{\omega}\bar{t}. \tag{4.30}$$

Then the eigenvalue problem can be written in the form

$$\begin{aligned}\bar{\omega}^2(-\bar{A}^2V - 2\bar{A}^{-1}\bar{B}V_s + V_{ss}) &= \bar{B}P - \bar{A}P_s \\ &+ t_0\big[V(-\bar{A}\bar{C} + \bar{B}^2) + V_s(8\bar{A}^{-3}\bar{B}^3 - 7\bar{A}^{-2}\bar{B}\bar{C} + \bar{A}^{-1}\bar{D} - \bar{A}\bar{B}) \\ &+ V_{ss}(-8\bar{A}^{-2}\bar{B}^2 + 3\bar{A}^{-1}\bar{C} - \bar{A}^2) + V_{sss}(4\bar{A}^{-1}\bar{B}) - V_{ssss}\big].\end{aligned} \tag{4.31}$$

Since the ends of the membrane have no motion in both tangential and radial directions, with the use of equation (4.12) the boundary conditions become

$$\begin{aligned}&V(0) = 0, \quad V_s(0) = 0, \\ &V(s_0) = 0, \quad V_s(s_0) = 0,\end{aligned} \tag{4.32}$$

where s_0 is the nondimensional perimeter length defined in equation (3.8).

4.3 Finite Difference Analysis

The boundary value problem, i.e., equations (4.31)-(4.32), can be solved numerically by using the finite difference technique. No general closed-form solution exists. The membrane is divided into a discrete system of points and at each internal point equations (4.31)-(4.32) are applied.

In the first place, let us write the fourth order differential equation in a more convenient form as

$$\begin{aligned}\bar{\omega}^2(f_1V + f_2V' + f_3V'') &= g_1P + g_2P' \\ &+ (f_4V + f_5V' + f_6V'' + f_7V''' + f_8V'''')\end{aligned} \tag{4.33}$$

where a prime denotes differentiation with respect to s and

$$
\begin{aligned}
f_1 &= -\overline{A}^2, \\
f_2 &= -2\overline{A}^{-1}\overline{B}, \\
f_3 &= 1, \\
f_4 &= t_0(-\overline{A}\,\overline{C} + \overline{B}^2), \\
f_5 &= t_0(8\overline{A}^{-3}\overline{B}^3 - 7\overline{A}^{-2}\overline{B}\,\overline{C} + \overline{A}^{-1}\overline{D} - \overline{A}\,\overline{B}), \\
f_6 &= t_0(-8\overline{A}^{-2}\overline{B}^2 + 3\overline{A}^{-1}\overline{C} - \overline{A}^2), \\
f_7 &= 4\overline{A}^{-1}\overline{B}t_0, \\
f_8 &= -t_0,
\end{aligned}
\qquad (4.34)
$$

$$
\begin{aligned}
g_1 &= \overline{B}, \\
g_2 &= -\overline{A}.
\end{aligned}
$$

We note that f_i and g_i are functions of the static membrane tension t_0 and angle ψ_0, which can be obtained from the equilibrium analysis of Chapter 3.

The membrane curve is divided into N sections and the numbering of nodes is shown in Fig. 4.2. The length of each membrane segment is denoted h. The subdivision of the base shown is needed for the calculation of the hydrodynamic pressure in a subsequent section. Discretizing equation (4.33), we have

$$
\begin{aligned}
\overline{\omega}^2 [(f_1)_i V_i + (f_2)_i V_i' + (f_3)_i V_i''] &= (g_1)_i P_i + (g_2)_i P_i' \\
&+ ((f_4)_i V_i + (f_5)_i V_i' + (f_6)_i V_i'' + (f_7)_i V_i''' + (f_8)_i V_i'''') , \quad \text{for } i = 2, \ldots, N .
\end{aligned}
\qquad (4.35)
$$

From the central difference concept, it is found that

$$
V_i' = \frac{1}{2h}(V_{i+1} - V_{i-1}), \qquad (4.36)
$$

$$
V_i'' = \frac{1}{h^2}(V_{i+1} - 2V_i + V_{i-1}), \qquad (4.37)
$$

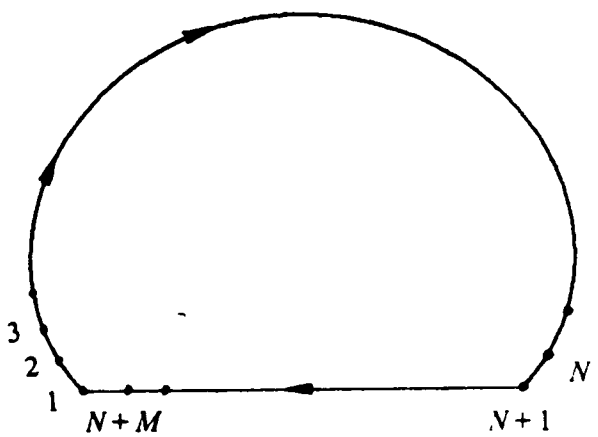

Fig. 4.2 Numbering of Nodes on the Boundary

$$V_i''' = \frac{1}{2h^3}(V_{i+2} - 2V_{i+1} + 2V_{i-1} - V_{i-2}), \tag{4.38}$$

$$V_i'''' = \frac{1}{h^4}(V_{i+2} - 4V_{i+1} + 6V_i - 4V_{i-1} + V_{i-2}). \tag{4.39}$$

Examining equations (4.36)-(4.39), it is seen that special manipulation is needed for some derivatives which require membrane displacement values outside the end points of the membrane. Making use of equation (4.36) for the first derivative of V, the four boundary conditions (4.32) for the discretized system become

$$\begin{aligned} &V_1 = 0, \quad V_2 = V_0, \\ &V_{N+1} = 0, \quad V_N = V_{N+2}. \end{aligned} \tag{4.40}$$

Substituting equations (4.36)-(4.39) and using (4.40), (4.35) can be written as

$$\bar{\omega}^2 \sum_{j=2}^{N} b_{i,j} V_j = \sum_{j=2}^{N} a_{i,j} V_j + (g_1)_i P_i + (g_2)_i P_i', \quad \text{for } i = 2, \ldots, N \tag{4.41}$$

where

$$\begin{aligned} &b_{i,j-1} = -(F_2)_i + (F_3)_i \qquad i = 3, \ldots, N, \\ &b_{i,j} = (F_1)_i - 2(F_3)_i \qquad i = 2, \ldots, N, \\ &b_{i,j+1} = (F_2)_i + (F_3)_i \qquad i = 2, \ldots, N-1, \\ &a_{i,j-2} = -(F_7)_i + (F_8)_i \qquad i = 4, \ldots, N, \\ &a_{i,j-1} = -(F_5)_i + (F_6)_i + 2(F_7)_i - 4(F_8)_i \quad i = 3, \ldots, N, \\ &a_{2,2} = (F_4)_2 - 2(F_6)_2 - (F_7)_2 + 7(F_8)_2, \\ &a_{i,j} = (F_4)_i - 2(F_6)_i + 6(F_8)_i \quad i = 3, \ldots, N-1, \\ &a_{N,N} = (F_4)_N - 2(F_6)_N + (F_7)_N + 7(F_8)_N, \\ &a_{i,j+1} = (F_5)_i + (F_6)_i - 2(F_7)_i - 4(F_8)_i \qquad i = 2, \ldots, N-1, \\ &a_{i,j+2} = (F_7)_i + (F_8)_i \qquad\qquad i = 2, \ldots, N-2, \end{aligned} \tag{4.42}$$

in which

$$F_1 = f_1, \quad F_2 = \frac{f_2}{2h}, \quad F_3 = \frac{f_3}{h^2},$$
$$F_4 = f_4, \quad F_5 = \frac{f_5}{2h}, \quad F_6 = \frac{f_6}{h^2}, \quad F_7 = \frac{f_7}{2h^3}, \quad F_8 = \frac{f_8}{h^4}, \tag{4.43}$$

and all the rest of $a_{i,j}$ and $b_{i,j}$ $(i, j = 2, \ldots, N)$ are zero.

It is seen that f_i given in equation (4.43) require information on t_0 and ψ_0 of the static analysis. t_0 is a constant along the membrane curve and does not need to be discretized, but the calculations of $\overline{A}, \overline{B}, \overline{C}$ and $\overline{D}$ in equation (4.34) for nodes 2 to N of the discretized membrane are still to be dealt with. Using the central difference technique, the values of $\overline{A}, \overline{B}, \overline{C}$ and $\overline{D}$ at node i can be approximated by

$$\overline{A}_i = \frac{1}{2h}[(\psi_0)_{i+1} - (\psi_0)_{i-1}], \tag{4.44}$$

$$\overline{B}_i = \frac{1}{h^2}[(\psi_0)_{i+1} - 2(\psi_0)_i + (\psi_0)_{i-1}], \tag{4.45}$$

$$\overline{C}_i = \frac{1}{2h^3}[(\psi_0)_{i+2} - 2(\psi_0)_{i+1} + 2(\psi_0)_{i-1} - (\psi_0)_{i-2}], \tag{4.46}$$

$$\overline{D}_i = \frac{1}{h^4}[(\psi_0)_{i+2} - 4(\psi_0)_{i+1} + 6(\psi_0)_i - 4(\psi_0)_{i-1} + (\psi_0)_{i-2}]. \tag{4.47}$$

The static analysis of Chapter 3 gives $(\psi_0)_j, j = 1, \ldots, N$. Examining the derivatives in equations (4.44)-(4.47), we observe that the evaluation of $\overline{C}$ and $\overline{D}$, at node 2 and N, require the use of $(\psi_0)_0$ and $(\psi_0)_{N+1}$, which are outside the membrane and cannot be determined. This difficulty is overcome by the added use of the forward difference and backward difference. At node 2, with the use of forward difference, the approximations of $\overline{C}$ and $\overline{D}$ are achieved by

$$\begin{aligned}\overline{C}_2 &\cong \frac{1}{h}(\overline{B}_3 - \overline{B}_2) \\ &\cong \frac{1}{h^3}[(\psi_0)_4 - 3(\psi_0)_3 + 3(\psi_0)_2 - (\psi_0)_1],\end{aligned} \tag{4.48}$$

$$\begin{aligned}\overline{D}_2 &\cong \frac{1}{h}(\overline{C}_3 - \overline{C}_2) \\ &\cong \frac{1}{h^4}[0.5(\psi_0)_5 - 2(\psi_0)_4 + 3(\psi_0)_3 - 2(\psi_0)_2 + 0.5(\psi_0)_1].\end{aligned} \tag{4.49}$$

It should be mentioned that $\overline{B}_2$, $\overline{B}_3$, and $\overline{C}_3$ in the above calculations are obtained from the central difference formula. Similarly, applying the backward difference to $\overline{C}$ and $\overline{D}$ for node N, we have

$$\begin{aligned}\overline{C}_N &\cong \frac{1}{h}(\overline{B}_N - \overline{B}_{N-1}) \\ &\cong \frac{1}{h^3}[(\psi_0)_{N+1} - 3(\psi_0)_N + 3(\psi_0)_{N-1} - (\psi_0)_{N-2}],\end{aligned} \tag{4.50}$$

$$\begin{aligned}\overline{D}_N &\cong \frac{1}{h}(\overline{C}_N - \overline{C}_{N-1}) \\ &\cong \frac{1}{h^4}[0.5(\psi_0)_{N+1} - 2(\psi_0)_N + 3(\psi_0)_{N-1} - 2(\psi_0)_{N-2} + 0.5(\psi_0)_{N-3}],\end{aligned} \tag{4.51}$$

where $\overline{B}_N$, $\overline{B}_{N-1}$ and $\overline{C}_{N-1}$ are calculated from the central difference.

Therefore, besides the approximations of special derivative equations (4.48)-(4.51), the majority of the approximations of derivatives $\overline{A}$, $\overline{B}$, $\overline{C}$ and $\overline{D}$ can be calculated by equations (4.44)-(4.47).

4.4 Hydrodynamic Pressures

The hydrodynamic pressures described in previous sections are calculated using the boundary element method. The boundary element method converts the two-dimensional potential flow problem into a one-dimensional integral equation, which involves only the velocity potential and its normal derivative on the boundary.

4.4.1 Problem Formulation

Under the assumption that the water is incompressible and inviscid, the motion of the water can be represented by the Laplace's equation

$$\nabla^2\phi = \frac{\partial^2\phi}{\partial X^2} + \frac{\partial^2\phi}{\partial Y^2} = 0 \tag{4.52}$$

where $\phi(X,Y,t)$ is the velocity potential. Since the normal velocity for the water particles along the base of the membrane dam should be zero,

$$\frac{\partial\phi}{\partial n} = \frac{\partial\phi}{\partial Y} = 0 \quad \text{on the base,} \tag{4.53}$$

in which n is the outward-pointing unit normal. Along the membrane surface, which is impenetrable, the normal velocity of the water is equal to that of the membrane element. We thus have

$$\frac{\partial\phi}{\partial n} = -w_t\,. \tag{4.54}$$

Using equation (4.12), we replace the normal displacement w in terms of the tangential displacement v in (4.54) and obtain

$$\frac{\partial\phi}{\partial n} = -A^{-1}v_{St}\,. \tag{4.55}$$

From Lamb [20], Bernoulli's equation for an incompressible fluid has the form

$$\frac{p}{\rho} = \phi_t + gY - \frac{1}{2}(\nabla\phi)^2 + F(t) \tag{4.56}$$

in which ρ and g are the density of the water and the acceleration of gravity, respectively, $F(t)$ is a time-dependent integration "constant" and $\nabla\phi$ is the resultant potential, which can be put in the form

$$\nabla\phi = \left[\left(\frac{\partial\phi}{\partial X}\right)^2 + \left(\frac{\partial\phi}{\partial Y}\right)^2\right]^{\frac{1}{2}}.$$

Since the value of $F(t)$ has no effect on p, as pointed out by Lamb, we can set it equal to the specific potential energy $(-gY)$. Moreover, in the perturbation of velocity, the $(\nabla\phi)^2$ in Bernoulli's equation becomes a second-order term and is neglected in our linear analysis. It follows that the hydrodynamic pressure is

$$p = \rho\phi_t . \tag{4.57}$$

It is required that we transform this potential problem using the nondimensional variables. Let us define

$$\begin{aligned} \phi &= \chi\bar{\phi}, \\ \rho &= \kappa\bar{\rho}, \end{aligned} \tag{4.58}$$

where χ and κ are unknown dimensional factors. Using the nondimensional variables introduced in section 4.2 and substituting equation (4.58) into (4.55) and (4.57), we have

$$\frac{\chi\partial\bar{\phi}}{L_0\partial\bar{n}} = -\frac{L_0\sqrt{\gamma}}{\sqrt{\mu}}\bar{A}^{-1}v_{s\bar{t}}, \tag{4.59}$$

$$\gamma L_0\bar{p} = \kappa\chi\frac{\sqrt{\gamma}}{\sqrt{\mu}}\bar{\rho}\bar{\phi}_{\bar{t}}, \tag{4.60}$$

in which we have used the nondimensional outward normal $\bar{n}$ such that

$$n = L_0\bar{n}. \tag{4.61}$$

The results of equations (4.59) and (4.60) lead to

$$\bar{\phi} = \frac{\sqrt{\mu}}{L_0^2\sqrt{\gamma}}\phi, \tag{4.62}$$

$$\bar{p} = \frac{L_0}{\mu}\, p\,. \tag{4.63}$$

Applying these nondimensional variables, therefore, the linearized boundary value problem becomes

$$\nabla^2 \bar{\phi} = 0 \qquad \text{on the water domain,} \tag{4.64}$$

$$\frac{\partial \bar{\phi}}{\partial \bar{n}} = -\bar{A}^{-1} v_{s\bar{t}} \quad \text{on the membrane,} \tag{4.65}$$

$$\frac{\partial \bar{\phi}}{\partial \bar{n}} = 0 \qquad \text{on the base,} \tag{4.66}$$

and equation (4.57) becomes

$$\bar{p} = \bar{\rho}\bar{\phi}_{\bar{t}}\,. \tag{4.67}$$

Since we consider only harmonic motion, as described in equations (4.29)-(4.30), we apply separation of variables for $\bar{\phi}$ and write

$$\bar{\phi}(s, \bar{t}) = \Phi(s) \sin \bar{\omega}\bar{t} \tag{4.68}$$

in which we represent $\bar{\phi}$ in terms of the membrane arc length s, rather than the Cartesian coordinates. Eliminating the time factor by the substitutions of equations (4.29)-(4.30) and (4.68), the potential problem is stated as

$$\nabla^2 \Phi = 0 \qquad \text{on the water domain,} \tag{4.69}$$

$$\frac{\partial \Phi}{\partial \bar{n}} = \bar{\omega}\bar{A}^{-1} V' \quad \text{on the membrane,} \tag{4.70}$$

$$\frac{\partial \Phi}{\partial \bar{n}} = 0 \qquad \text{on the base,} \tag{4.71}$$

where a prime denotes differentiation with respect to s. Also, the hydrodynamic pressure is

$$P = \overline{\omega\rho}\Phi\,. \tag{4.72}$$

4.4.2 Boundary Element Method

The potential problem described in equations (4.69)-(4.72) is solved using the boundary element method, which is based on Green's function. Let us suppose that Ω denotes the water domain inside the membrane and Γ the boundary domain, which includes the membrane curve and the base. Applying the free space Green's function, G, of Laplace's equation, we can obtain the integral equation

$$\int_\Gamma \left[\Phi(s)\,\frac{\partial G}{\partial \bar{n}}\,ds - \frac{\partial \Phi(s)}{\partial \bar{n}}\,G\right] ds = \alpha(\tilde{s})\,\Phi(\tilde{s}) \tag{4.73}$$

in which

$$\begin{aligned} &\tilde{s} \in \Omega + \Gamma\,, \quad s \in \Gamma\,, \\ &G = \log\,|\text{length from } s \text{ to } \tilde{s}\,| = \log\,|s - \tilde{s}\,|\,, \end{aligned} \tag{4.74}$$

and

(i) if $\tilde{s} \in \Omega$ then $\alpha = 2\pi$,

(ii) if $\tilde{s} \in \Gamma$ then α is the internal angle at $\tilde{s}$.

Substituting the boundary conditions (4.70) and (4.71) into equation (4.73), it is possible to solve for the unknown velocity potential Φ on the boundary. However, for the Neumann problem ($\partial\Phi/\partial\bar{n}$ is given on all of Γ) [21] a complementary condition

$$\int_\Gamma \Phi(s)\,ds = 0 \tag{4.75}$$

must be imposed to ensure a unique solution for Φ.

The boundary Γ is subdivided into intervals as shown in Fig. 4.2, in which the membrane contains N segments and the base has M segments. Linear approximations are employed for Φ and $\partial\Phi/\partial\bar{n}$ on each element. Thus, on each straight line interval Γ_j, connected between nodal points j and $j+1$, the values of Φ and $\partial\Phi/\partial\bar{n}$ are

$$\Phi = (1-\xi)\Phi_j + \xi\Phi_{j+1}\,, \tag{4.76}$$

$$\frac{\partial\Phi}{\partial\bar{n}} = (1-\xi)\frac{\partial\Phi_j}{\partial\bar{n}} + \xi\frac{\partial\Phi_{j+1}}{\partial\bar{n}}\,, \tag{4.77}$$

where ξ is a linear interpolation function which is zero at node j and is unity at node $j+1$. Applying equation (4.73) at each node of the boundary and using equations (4.76)-(4.77), we have

$$\begin{aligned}\sum_{j=1}^{N+M}\left[\Phi_j\int_{\Gamma_j}(1-\xi)\frac{\partial G}{\partial\bar{n}}\,ds + \Phi_{j+1}\int_{\Gamma_j}\xi\frac{\partial G}{\partial\bar{n}}\,ds\right]\\ -\sum_{j=1}^{N+M}\left[\frac{\partial\Phi_j}{\partial\bar{n}}\int_{\Gamma_j}(1-\xi)G\,ds + \frac{\partial\Phi_{j+1}}{\partial\bar{n}}\int_{\Gamma_j}\xi G\,ds\right]\\ = \alpha_i\Phi_i\,, \qquad i = 1,\ldots,N+M\end{aligned} \tag{4.78}$$

in which now $G = \log r = \log|s-\tilde{s}_i|$ and $\int_{\Gamma_j}$ denotes integration over the interval Γ_j. Instead of using a numerical quadrature formula for approximate evaluations, Ingham, Heggs and Manzoon [22] presented analytical expressions for the exact evaluations of the integrals in equation (4.78).

Consider the boundary element Γ_j with a point source at node i, as shown in Fig. 4.3. Let $\hat{h}$ denote the length of the interval and a and b denote the distances of node i from nodes j and $j+1$, respectively. The following expressions are given in [22] :

$$\int_{\Gamma_j}\frac{\partial G}{\partial\bar{n}}\,ds = I_1\,, \tag{4.79}$$

$$\int_{\Gamma_j} G ds = J_1 , \tag{4.80}$$

$$\int_{\Gamma_j} \xi \frac{\partial G}{\partial \bar{n}} ds = \frac{1}{\hat{h}} (a \cos \beta I_1 + I_2) , \tag{4.81}$$

$$\int_{\Gamma_j} \xi G ds = \frac{1}{\hat{h}} (a \cos \beta J_1 + J_2) , \tag{4.82}$$

where

$$I_1 = \psi , \tag{4.83a}$$

$$I_2 = a \sin \beta (\log b - \log a) , \tag{4.83b}$$

$$J_1 = a \cos \beta (\log a - \log b) + \hat{h} (\log b - 1) + a\psi \sin \beta , \tag{4.83c}$$

$$J_2 = \frac{1}{2} (b^2 \log b - a^2 \log a) - \frac{1}{4} (b^2 - a^2) , \tag{4.83d}$$

and ψ and β are calculated by

$$\psi = \measuredangle \cos \left(\frac{a^2 + b^2 - \hat{h}^2}{2ab} \right) , \quad 0 \le \psi \le \pi , \tag{4.84}$$

$$\beta = \measuredangle \cos \left(\frac{a^2 + \hat{h}^2 - b^2}{2a\hat{h}} \right) , \quad 0 \le \beta \le \pi , \tag{4.85}$$

In equation (4.83), we notice that special cases arise if either a or b is zero. In both cases, the values of I_1 and I_2 are equal to zero and [23]

$$J_1 = \hat{h}(\log \hat{h} - 1) .$$

However, if $a = 0$,

$$J_2 = -\hat{h}^2(\frac{1}{4} - \frac{1}{2}\log \hat{h}) ;$$

and if $b = 0$,

$$J_2 = \hat{h}^2(\frac{1}{4} - \frac{1}{2}\log \hat{h}) .$$

Furthermore, if nodes i, j and $j+1$ are collinear (i.e., $\beta = 0$ or $\beta = \pi$), it is found that I_1 and I_2 are both zero and the formula for J_1 in equation (4.83) can be simplified to the following :

if $\beta = 0$,

$$J_1 = a(\log a - 1) - b(\log b - 1) ;$$

if $\beta = \pi$,

$$J_1 = a(1 - \log a) + b(\log b - 1) .$$

Therefore, the linear algebraic equation can be expressed in matrix form as

$$[R]_{(N+M)\times(N+M)} \{\Phi\}_{(N+M)\times 1} = [L]_{(N+M)\times(N+M)} \left\{ \frac{\partial \Phi}{\partial \bar{n}} \right\}_{(N+M)\times 1} \tag{4.86}$$

where

$$R_{i,j} = \left\{ I_1 - \frac{1}{\hat{h}}(a\cos\beta I_1 + I_2) - \delta_{ij}\alpha_i \right\}_{\Gamma_j} + \left\{ \frac{1}{\hat{h}}(a\cos\beta I_1 + I_2) \right\}_{\Gamma_{j-1}} ,$$

$$L_{i,j} = \left\{ J_1 - \frac{1}{\hat{h}}(a\cos\beta J_1 + J_2) \right\}_{\Gamma_j} + \left\{ \frac{1}{\hat{h}}(a\cos\beta J_1 + J_2) \right\}_{\Gamma_{j-1}} ,$$

δ_{ij} denotes the Kronecker delta, and the subscript Γ_j outside the { } indicates the use of the element Γ_j for the computations inside the { }. We notice that when $j = 1$, $\Gamma_{N+M} = \Gamma_{j-1}$.

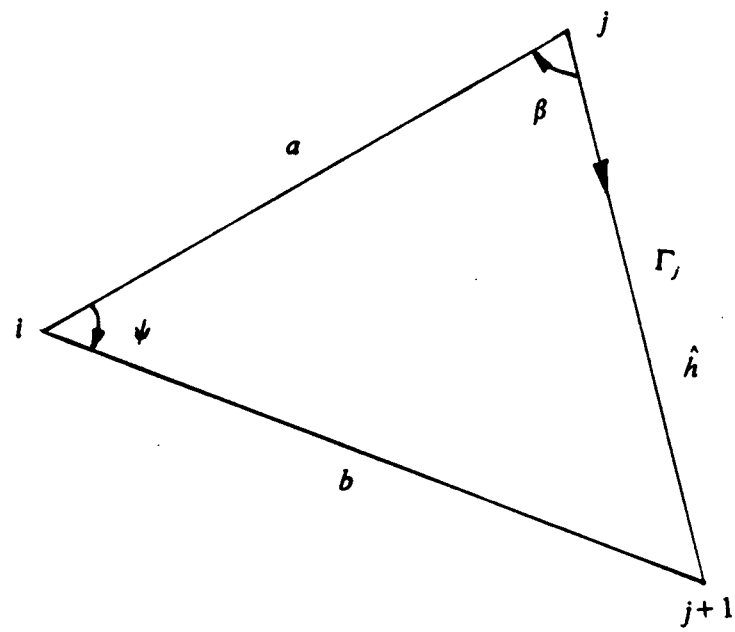

Fig. 4.3 Straight Line Element Geometry

Since our problem is of Neumann type, the additional condition (4.75) must be imposed. Using the linear approximation for Φ and equation (4.75), we have

$$\sum_{j=1}^{N+M} \left\{ \Phi_j \int_{\Gamma_j} (1-\xi) ds + \Phi_{j+1} \int_{\Gamma_j} \xi ds \right\} = 0 .$$

Then,

$$\sum_{j=1}^{N+M} \left\{ \Phi_j \frac{\hat{h}_{(j)}}{2} + \Phi_{j+1} \frac{\hat{h}_{(j)}}{2} \right\} = 0 \tag{4.87}$$

where the subscript (j) of $\hat{h}$ indicates the boundary element involved. The addition of equation (4.87) to (4.86) as the last algebraic equation forms a new matrix system,

$$[\tilde{R}]\{\Phi\} = [\tilde{L}] \left\{ \frac{\partial \Phi}{\partial \bar{n}} \right\} \tag{4.88}$$

in which both $[\tilde{R}]$ and $[\tilde{L}]$ are of order $(N+M+1) \times (N+M)$. From equation (4.87) the coefficients in the last rows of $[\tilde{R}]$ and $[\tilde{L}]$ are

$$\tilde{R}_{N+M+1,j} = \frac{\hat{h}_{(j)}}{2} + \frac{\hat{h}_{(j-1)}}{2} , \quad j = 1, \ldots, N+M ,$$

$$\tilde{L}_{N+M+1,j} = 0 , \quad j = 1, \ldots, N+M ,$$

in which we note when $j = 1$, $(N+M) = (j\text{-}1)$. Substituting the boundary conditions into equation (4.88) and arranging the known boundary conditions on the right hand side, we can then solve for the missing boundary information. We note that $[\tilde{R}]$ and $[\tilde{L}]$ are rectangular matrices, and the matrix operation can be achieved in a least-squares sense.

4.4.3 Application

Discretizations of the boundary conditions (4.70) and (4.71) lead to

$$\frac{\partial \Phi_i}{\partial \bar{n}} = \bar{\omega} \bar{A}_i^{-1} V_i', \qquad i = 1, \ldots, N+1, \tag{4.89}$$

$$\frac{\partial \Phi_i}{\partial \bar{n}} = 0, \qquad i = N+2, \ldots, N+M. \tag{4.90}$$

Equation (4.88) then can be manipulated such that

$$\{\Phi\}_{(N+M)\times 1} = [CC]_{(N+M)\times(N+M)} \left\{ \frac{\partial \Phi}{\partial \bar{n}} \right\}_{(N+M)\times 1} \tag{4.91}$$

in which

$$[CC] = [\tilde{R}]^{-1} [\tilde{L}].$$

We now proceed by separating $\{\Phi\}$ in equation (4.91) into two submatrices, $\{\Phi_m\}$ and $\{\Phi_b\}$. Let $\{\Phi_m\}$ and $\{\Phi_b\}$ represent the velocity potential on the membrane and on the base, respectively. In a similar manner, separate $\{\partial\Phi/\partial\bar{n}\}$ into $\{\partial\Phi_m/\partial\bar{n}\}$ and $\{\partial\Phi_b/\partial\bar{n}\}$. Then equation (4.91) can be expressed as

$$\begin{Bmatrix} \{\Phi_m\} \\ \{\Phi_b\} \end{Bmatrix} = \begin{bmatrix} [CC_{11}] & [CC_{12}] \\ [CC_{21}] & [CC_{22}] \end{bmatrix} \begin{Bmatrix} \{\partial\Phi_m/\partial\bar{n}\} \\ \{\partial\Phi_b/\partial\bar{n}\} \end{Bmatrix}.$$

Since we only need $\{\Phi\}_m$, expanding this and noting equation (4.90) we have

$$\{\Phi_m\}_{(N+1)\times 1} = [CC_{11}]_{(N+1)\times(N+1)} \left\{ \frac{\partial \Phi_m}{\partial \bar{n}} \right\}_{(N+1)\times 1}. \tag{4.92}$$

Applying equation (4.89), and using (4.36) and the boundary conditions (4.40), we can construct a coefficient matrix $[TM]$ such that

$$\{\Phi_m\}_{(N+1)\times 1} = [CC_{11}]\,[TM]\,\overline{\omega}\begin{Bmatrix} 0 \\ \{v\} \\ 0 \end{Bmatrix} = \overline{\omega}[PD]_{(N+1)\times(N+1)}\begin{Bmatrix} 0 \\ \{v\} \\ 0 \end{Bmatrix}_{(N+1)\times 1} \tag{4.93}$$

in which

$$TM_{1,1} = -\frac{\overline{A}_1^{-1}}{h},$$

$$TM_{1,2} = \frac{\overline{A}_1^{-1}}{h},$$

$$TM_{j,j-1} = -\frac{\overline{A}_j^{-1}}{2h}, \quad j = 2, \ldots, N,$$

$$TM_{j,j+1} = \frac{\overline{A}_j^{-1}}{2h}, \quad j = 2, \ldots, N,$$

$$TM_{N+1,N} = -\frac{\overline{A}_{N+1}^{-1}}{h},$$

$$TM_{N+1,N+1} = \frac{\overline{A}_{N+1}^{-1}}{h}.$$

All the rest of $TM_{i,j}(i, j = 1, \ldots, N+1)$ are zero and h is the length of the membrane element as defined previously. The evaluations of $\overline{A}_1$ and $\overline{A}_{N+1}$ can be obtained by applying forward and backward differences, respectively, in a similar manner to that described in Section 4.3.

Discretizing equation (4.72), the hydrodynamic pressure on the membrane can be written as

$$\{P\}_{(N+1)\times 1} = \overline{\omega}^2\overline{\rho}\,[PD]_{(N+1)\times(N+1)}\begin{Bmatrix} 0 \\ \{v\} \\ 0 \end{Bmatrix}_{(N+1)\times 1}. \tag{4.94}$$

Therefore, considering the hydrodynamic pressure P from node 2 to node N and expanding (4.94), we obtain

$$P_i = \overline{\omega}^2\overline{\rho}\,PD_{i,j}V_j, \quad i, j = 2, \ldots, N. \tag{4.95}$$

The hydrodynamic pressure derivative on the membrane is calculated using the central difference concept. Hence

$$\begin{aligned} P_i' &= \overline{\omega}^2 \overline{\rho}\, TN_{i,k}\, PD_{k,j}\, V_j \\ &= \overline{\omega}^2 \overline{\rho}\, PE_{i,j}\, V_j, \qquad i,j = 2, \ldots, N; \quad k = 1, \ldots, N+1 \end{aligned} \tag{4.96}$$

in which

$$\begin{aligned} TN_{i,j-1} &= -\frac{1}{2h}, \quad i = 2, \ldots, N, \\ TN_{i,j+1} &= \frac{1}{2h}, \qquad i = 2, \ldots, N. \end{aligned}$$

Substituting equations (4.95) and (4.96) into (4.41), the resulting eigenvalue problem of the free vibrations of the water-inflated membrane is

$$\overline{\omega}^2 \sum_{j=2}^{N} [b_{i,j} - \overline{PD}_{i,j} - \overline{PE}_{i,j}] V_j = \sum_{j=2}^{N} a_{i,j} V_j, \qquad \text{for } i = 2, \ldots, N \tag{4.97}$$

in which

$$\begin{aligned} \overline{PD}_{i,j} &= \overline{\rho}\,(g_1)_i\, PD_{i,j}, \\ \overline{PE}_{i,j} &= \overline{\rho}\,(g_2)_i\, PE_{i,j}, \end{aligned}$$

and g_1 and g_2 are defined in equation (4.34).

4.5 Numerical Results

4.5.1 Computer Programming

A complete computer program is written to determine the eigenvalues and eigenvectors of the water-inflated membrane. The static shape is obtained using the method described in Chapter 3. We note that at present the static shape is symmetric; on account of that, a small subroutine SYM

is created for the purpose of smoothing the data points which are obtained from the static analysis and making the shape exactly symmetric. This provides one way of checking and correcting programming errors when unreasonable results are obtained.

The constructions of $b_{i,j}$ and $a_{i,j}$ in equation (4.97) are straightforward as described in Sec. 4.3. Since the membrane shape is made exactly symmetric, $b_{i,j}$ and $a_{i,j}$ are symmetric matrices. The formation of the coefficient matrices, i.e., $[\tilde{R}]$ and $[\tilde{L}]$ in equation (4.88), using the boundary element method, for the evaluation of the hydrodynamic pressure is more complicated and must be carried out with caution. The fundamental programming structure of these matrices follows the computer program GM8 presented in the last chapter of Liggett and Liu [24], but is modified such that the calculations in Subsection 4.4.2 are used. These coefficient matrices are non-symmetric and fully-populated matrices which follow the essence of the boundary element method. Nevertheless, if we examine the first $(N+1) \times (N+1)$ elements of $[\tilde{R}]$ and $[\tilde{L}]$, they appear to be symmetric because of the symmetric static shape. The inverse of the rectangular matrix $[\tilde{R}]$ in equation (4.91) is completed using a subroutine LGINF from IMSL. The eigenvalue problem posed in equation (4.97) is solved using the EIGZF subroutine in IMSL.

The accuracy of the results depends upon the number of intervals used in the boundary domain. A convergence test is conducted in order to choose a suitable number of segments of the boundary domain, such that the stability of the numerical results is ensured. We assume that the perimeter length s_0 and the internal water head h_i of the water-inflated membrane are 2.5 and 2.0, respectively. The parameter $\overline{\rho}$ is assumed to be 1 for this convergence test. The first four eigenvalues are computed and listed in Table 4.1 for various numbers of intervals on the membrane curve and the base. We note that the results become more accurate as the number of intervals N of the membrane increases. However, increasing the number of intervals M of the base influences the results insignificantly. The two values $N = 61$ and $M = 11$ are chosen to obtain the results in subsequent subsections.

Referring to Brebbia [18], the discontinuities of the potential at both ends of the membrane can be treated using double-node representations. Each of these two nodes has a different boundary property, which depends on the location of the node. However, for these obtuse corners, it can

be shown that the results of this scheme are only slightly improved when small elements are used along the boundary.

4.5.2 Results

The effects of the parameters of the membrane and the relative densities of the membrane and water on the natural frequencies of the water-inflated membrane are examined numerically. The results are presented in figures and the first four eigenvalues, λ, which are equal to $\overline{\omega}^2$, are shown. Typical mode shapes are shown in Fig. 4.4, and are similar to those of the air-inflated membrane.

A model experiment was conducted to find the first two eigenvalues for different internal water heads. The length of the cylindrical membrane along the generators was 175.3 cm, while the base length L_0 and the perimeter S_0 of the membrane were 17.8 cm and 78.0 cm, respectively. The membrane mass per unit area was equal to 0.0627 gm/cm^2. Three different internal water heads, H_i, were used: (i) 46.7 cm, (ii) 68.1 cm, (iii) 88.4 cm. From the experiment, the corresponding natural frequencies were

(i) $\omega_1 = 11.2$ sec^{-1}, $\omega_2 = 15.7$ sec^{-1},

(ii) $\omega_1 = 12.6$ sec^{-1}, $\omega_2 = 28.6$ sec^{-1},

(iii) $\omega_1 = 15.7$ sec^{-1}, $\omega_2 = 27.3$ sec^{-1}.

The corresponding theoretical numerical results for the above membrane are

(i) $\omega_1 = 8.15$ sec^{-1}, $\omega_2 = 16.30$ sec^{-1},

(ii) $\omega_1 = 10.60$ sec^{-1}, $\omega_2 = 22.75$ sec^{-1},

(iii) $\omega_1 = 12.58$ sec^{-1}, $\omega_2 = 27.71$ sec^{-1}.

Considering the crudeness of the experiment, it is fair to say that the numerical results agree well with those of the experiment.

The experimental results are marked in Fig. 4.5, which also gives the first four λ values for h_i ranging from 2.2 to 5. If s_0 is equal to 2.5, the results are shown in Fig. 4.6 for h_i ranging from 1 to 4. We note that the water density ρ is equal to 1000 kg/m^3. This value is used in equation (4.63) to yield $\overline{\rho}$, which has the value of 283.42. In view of Figs. 4.5 and 4.6, an increase of the internal water head results in an increase of the natural frequencies.

N	M	λ_1	λ_2	λ_3	λ_4
25	21	0.8183	3.7595	10.3046	19.0817
51	11	0.8360	3.8397	10.5492	19.6298
51	21	0.8362	3.8412	10.5524	19.6353
51	31	0.8362	3.8420	10.5536	19.6378
61	11	0.8377	3.8475	10.5731	19.6828
61	21	0.8378	3.8488	10.5757	19.6872
61	31	0.8379	3.8495	10.5767	19.6893
71	11	0.8387	3.8522	10.5877	19.7151
71	21	0.8388	3.8533	10.5899	19.7188

Table 4.1 Test of Convergence Using $s_0 = 2.5$, $h_i = 2.0$, $h_w = 0.0$, and $\overline{\rho} = 1$

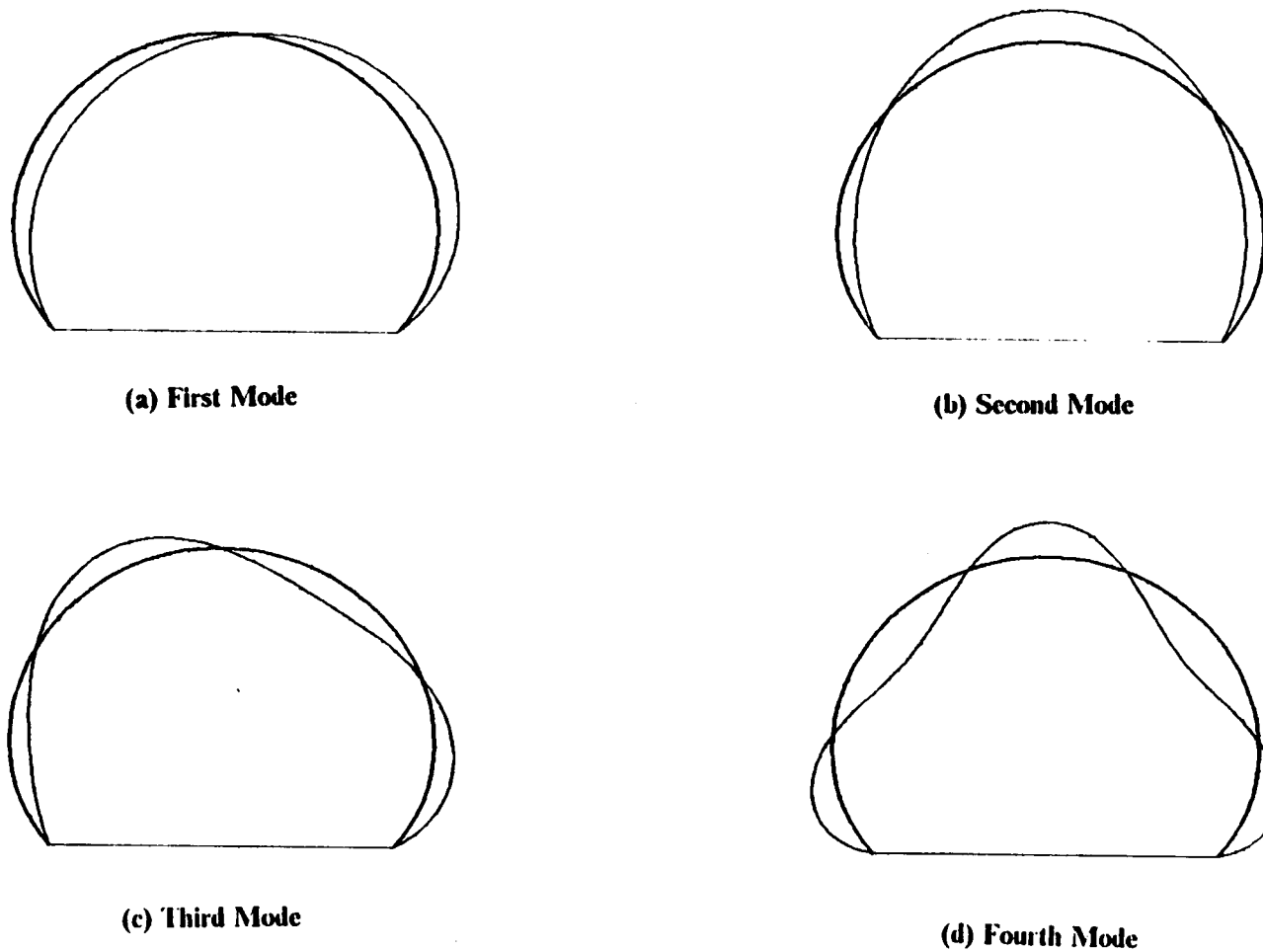

(a) First Mode

(b) Second Mode

(c) Third Mode

(d) Fourth Mode

Fig. 4.4 First Four Mode Shapes of Water-Inflated Membrane

The effect of the membrane mass can be shown to be insignificant by ignoring $b_{i,j}$ in equation (4.97). Using case (iii) of the experiment as an example, the natural frequencies, after neglecting the membrane mass, become $\omega_1 = 12.67$ sec^{-1} and $\omega_2 = 27.84$ sec^{-1}. However, this effect is included in our dynamic analysis.

Two different values of h_i, (i) 2.0 and (ii) 4.0, are considered in examining the effect of the perimeter length as shown in Figs. 4.7 and 4.8. $\overline{\rho}$ is assumed to be 283.42. It is seen that the eigenvalues increase rapidly as S_0 becomes closer to L_0, which corresponds to s_0 approaching 1.

The effect of the relative densities, in terms of the parameter $\overline{\rho}$, is examined first by considering two cases: (a) $s_0 = 2.5$, $h_i = 2.0$, (b) $s_0 = 4.0$, $h_i = 4.0$. It is noted that $\overline{\rho}$ is a function of the dimensional parameters L_0, μ and ρ as shown in equation (4.63), in which μ is the mass per unit length of the membrane (for a unit width). For $\overline{\rho}$ ranging from 0 to 500, the results are shown in Fig. 4.9 and Fig. 4.10 for case (a) and case (b), respectively. It is observed that λ becomes larger as $\overline{\rho}$ decreases.

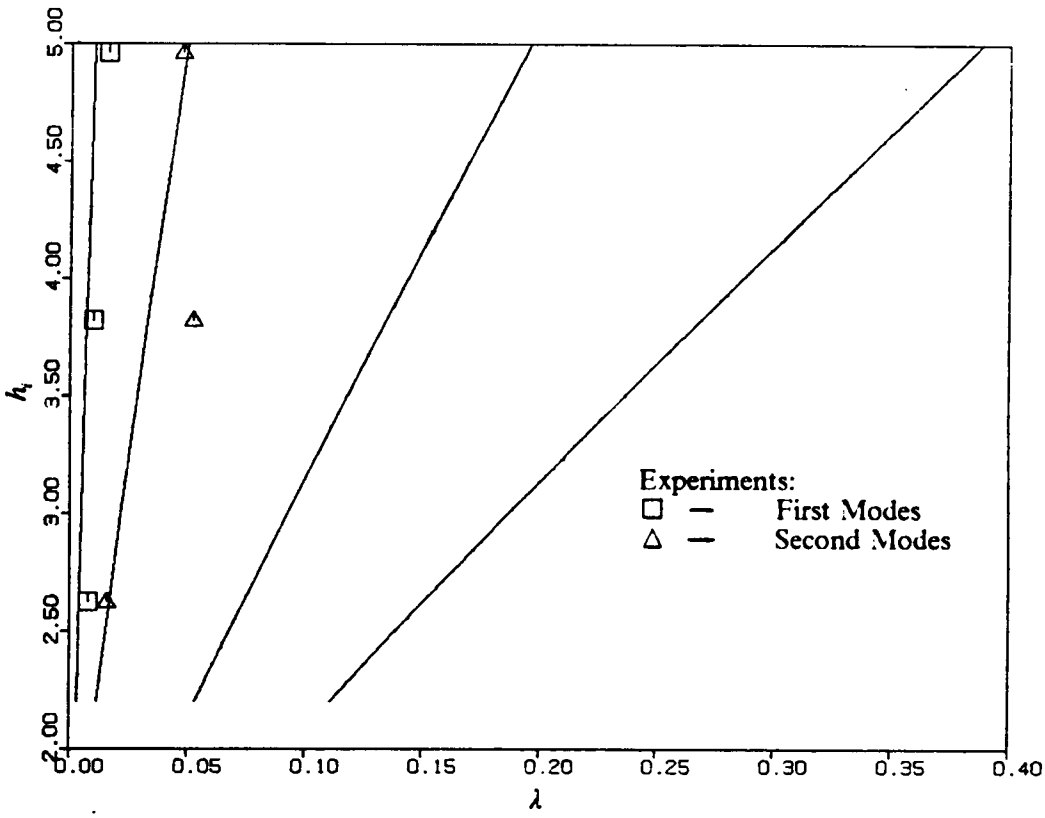

Fig. 4.5 h_i vs. λ for $s_0 = 4.39$ and $\bar{\rho} = 283.42$

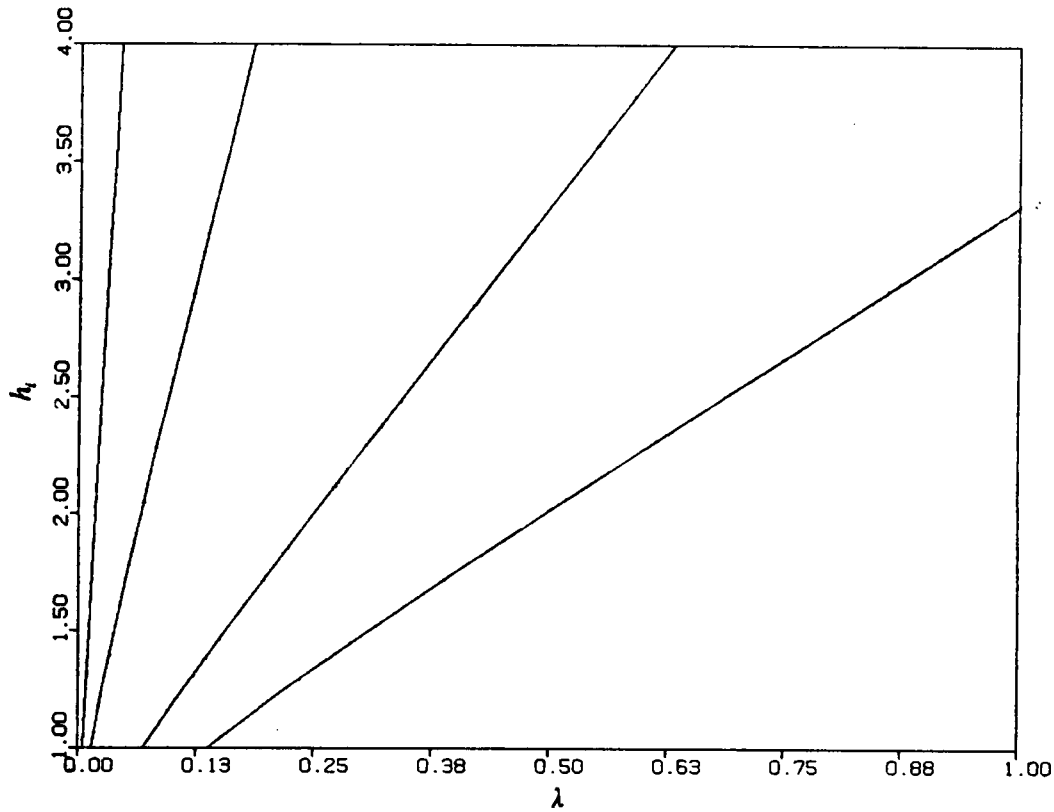

Fig. 4.6 h_1 **vs.** λ **for** $s_0 = 2.5$ **and** $\bar{\rho} = 283.42$

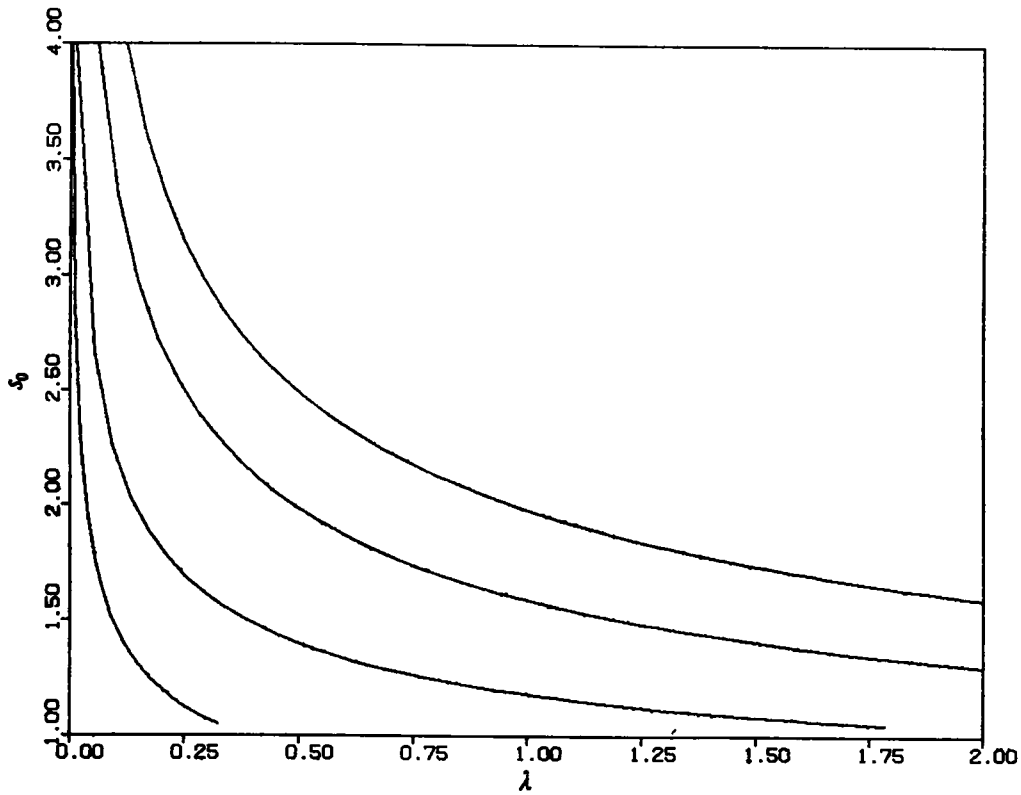

Fig. 4.7 s_0 **vs.** λ **for** $h_1 = 2.0$ **and** $\bar{\rho} = 283.42$

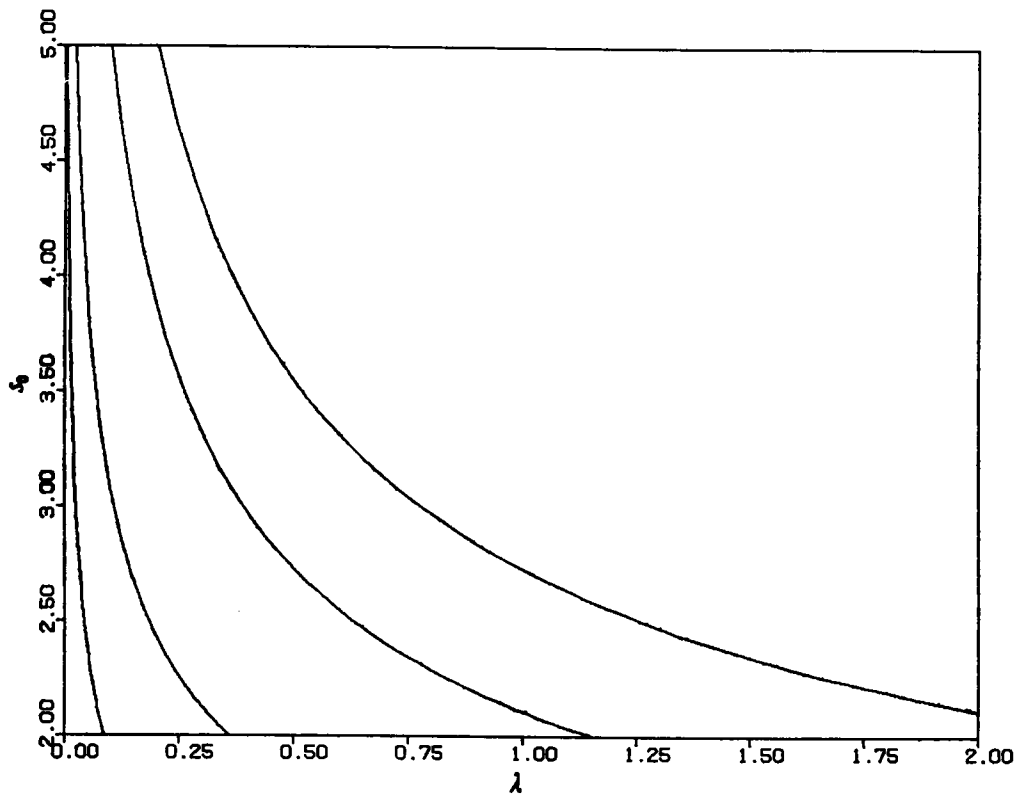

Fig. 4.8 s_0 **vs.** λ **for** $h_1 = 4.0$ **and** $\bar{\rho} = 283.42$

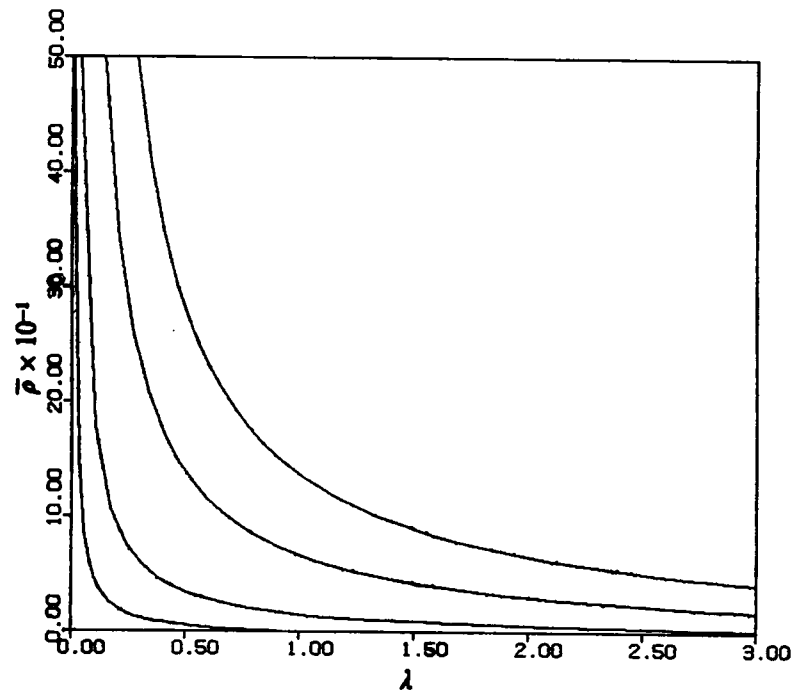

Fig. 4.9 $\bar{\rho}$ vs. λ for $s_0 = 2.5$ and $h_1 = 2.0$

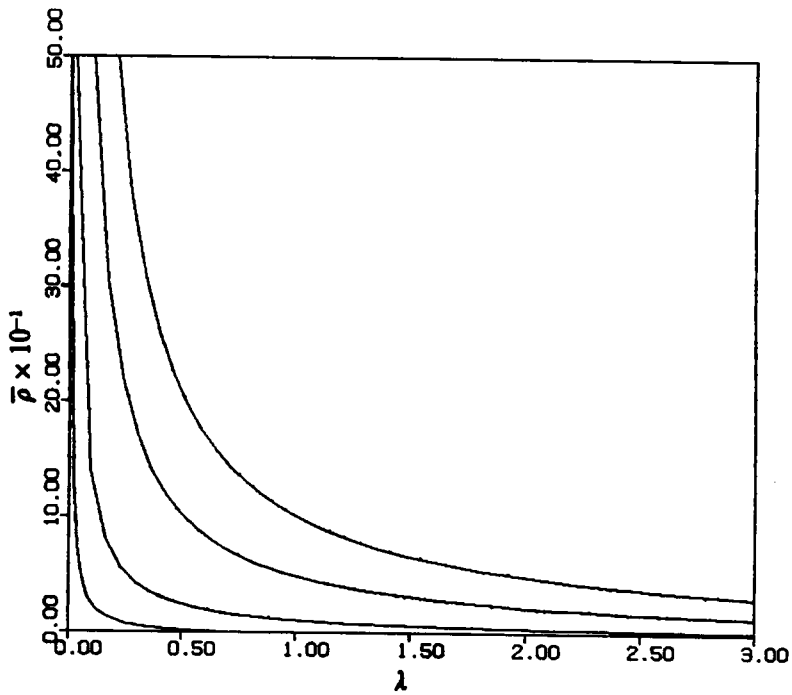

Fig. 4.10 $\bar{\rho}$ **vs.** λ **for** $s_0 = 4.0$ **and** $h_1 = 4.0$

Chapter 5

VIBRATIONS OF WATER-INFLATED DAM WITH AN UPSTREAM HEAD

This chapter deals with the free vibrations of a water-inflated dam with impounding water on the upstream side. Using the same terminology and derivations as in Chapter 4, we can arrive at a similar eigenvalue equation to that in equation (4.97), i.e.,

$$\overline{\omega}^2 \sum_{j=2}^{N} \left[b_{i,j} - \overline{PD}_{i,j} - \overline{PE}_{i,j} \right] V_j = \sum_{j=2}^{N} a_{i,j} V_j, \quad \text{for } i = 2, \ldots, N, \tag{5.1}$$

except that in the last two terms of the left hand bracket we have to include the pressure resulting from the vibrations of the upstream exterior water domain. The exterior hydrodynamic pressure is treated in this chapter.

The applications of boundary element methods in the studies of seismic responses of rigid and elastic dams impounding water on the upstream sides appeared in [25-28]; however, none of these works involved the investigation of the free vibration behavior. Shingu and Nishimura [29] studied

the free vibrations of immersed conical shells numerically by the finite element method and the results agreed well with experimental values.

Here, the exterior hydrodynamic pressure is treated using the boundary element method described in Section 4.4. The advantage of the use of the boundary element method over other domain methods, such as finite element methods, becomes evident, since only the boundary information is required.

In addition to the assumptions made on the membrane and the water in Chapter 4, the motion of the water is assumed to be small, and the effect of waves at the free surface of the impounded water is neglected. The upstream base, as well as the membrane base, is flat. The fictional boundary of the infinite domain is vertical, as illustrated in Fig. 5.1.

A subroutine is written to deal with the external pressure. Effects of the internal water head, impounding water height, and relative water density are examined.

5.1 Problem Formulation

To find the external hydrodynamic pressure acting on the membrane, we apply a similar approach to that in the previous chapter, by first formulating the two-dimensional potential flow problem. Again, the dimensionless Laplace's equation of the exterior water domain is

$$\nabla^2 \overline{\phi}_e = 0 \tag{5.2}$$

in which $\overline{\phi}_e$ is the velocity potential of the exterior domain. The corresponding boundary condition on the base is

$$\frac{\partial \overline{\phi}_e}{\partial \overline{n}_e} = 0, \tag{5.3}$$

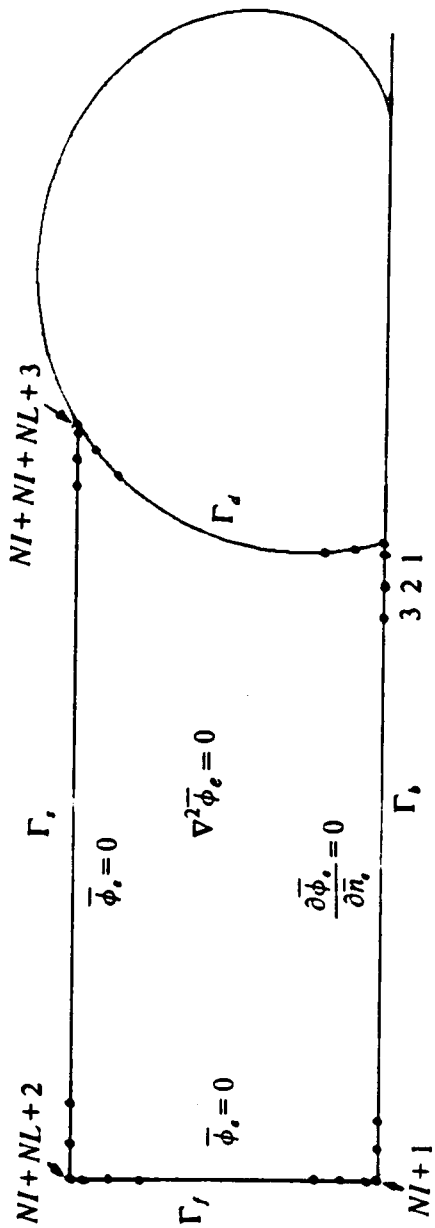

Fig. 5.1 Geometry of Exterior Potential Problem

A vertical fictitious boundary is assumed at the far end of the infinite domain, and the hydrodynamic pressure of the water is zero; thus, using Bernoulli's equation, which relates the pressure and velocity potential, on the fictitious boundary, we have

$$\bar{\phi}_e = 0. \tag{5.4}$$

On the other hand, at this boundary we can put the velocity of the water motion equal to zero by letting

$$\frac{\partial \bar{\phi}_e}{\partial \bar{n}_e} = 0.$$

Nevertheless, the distinction of the choice become insignificant as the distance of the fictitious boundary from the membrane is increased to several times larger than the base length L_0, and equation (5.4) is used for the condition on the fictitious boundary.

Since the displacements on the free surface are small, i.e., the effect of the surface waves is disregarded, the hydrodynamic pressure on the free surface is also zero; thus, on the free surface we have

$$\bar{\phi}_e = 0. \tag{5.5}$$

On the interaction boundary we have

$$\frac{\partial \bar{\phi}_e}{\partial \bar{n}_e} = \bar{A}^{-1} v_{s\bar{t}}. \tag{5.6}$$

It is important to note that the outward normal $\bar{n}_e$ is defined with respect to the exterior domain, and the definition of the direction of the membrane displacement v is unchanged from that of Chapter 4; therefore, equation (5.6) is different from (4.65) in sign.

Then, considering harmonic motion, we write

$$\bar{\phi}_e(s, \bar{t}) = \Phi_e(s) \sin \bar{\omega} \bar{t},$$

and after dropping the time factors in equations (5.2)-(5.6), we can write the boundary problem as

$$\nabla^2 \Phi_e = 0 \qquad \text{on the exterior domain,} \tag{5.7}$$

and the corresponding boundary conditions are

$$\frac{\partial \Phi_e}{\partial \bar{n}_e} = 0 \qquad \text{on the base,} \tag{5.8}$$

$$\Phi_e = 0 \qquad \text{on the free surface and fictitious boundary,} \tag{5.9}$$

$$\frac{\partial \bar{\Phi}_e}{\partial \bar{n}_e} = -\bar{\omega}\bar{A}^{-1}V' \qquad \text{on the membrane.} \tag{5.10}$$

The relationship between the external hydrodynamic pressure and velocity potential is

$$P_e = \bar{\omega}\bar{\rho}\bar{\Phi}_e, \tag{5.11}$$

which is the same as equation (4.72), but the direction of P_e defined here is opposite to that of P.

5.2 Application of Boundary Element Method

The formulation of the boundary element method to solve the Laplace's potential problem is given explicitly in Subsection 4.4.2, and the linear interpolation functions for the velocity potential and its derivative are again employed. For the interior water domain the Neumann condition, i.e., equation (4.75), is unchanged and imposed; but for the exterior domain, no additional equation is required because it has mixed boundary conditions, as described in equations (5.8)-(5.10).

The procedure for the attainment of the interior hydrodynamic pressure is the same here as described in Subsection 4.4.3 and is not repeated; a parallel technique is used in treating the hydrodynamic pressure for the exterior domain.

The exterior computational domain is comprised of the upstream bottom Γ_b, the fictitious vertical boundary Γ_f, the free surface Γ_s, and the upstream dam face Γ_d as shown in Fig. 5.1. The

velocity potential and its derivative for each boundary component are defined by adding the appropriate subscripts. Discretizing the boundary domain and using the boundary element method, we set up a system of algebraic equations for the Laplace's equation (5.7) as

$$[R]\{\Phi_e\} = [L]\left\{\frac{\partial \Phi_e}{\partial \bar{n}_e}\right\}. \tag{5.12}$$

For simplicity's sake, no subscript is added for these new coefficient matrices, i.e., $[R]$ and $[L]$, and compared to equation (4.88), no auxiliary condition is needed since this exterior potential problem has mixed boundary conditions. Therefore, $[R]$ and $[L]$ are square matrices.

Discretized forms of the boundary equations (5.8)-(5.10) are

$$\left(\frac{\partial \Phi_e}{\partial \bar{n}_e}\right)_l = 0 \qquad \text{on } \Gamma_b, \tag{5.13}$$

$$(\Phi_e)_l = 0 \qquad \text{on } \Gamma_f \text{ and } \Gamma_s, \tag{5.14}$$

$$\left(\frac{\partial \Phi_e}{\partial \bar{n}_e}\right)_l = -\bar{\omega}\bar{A}_l^{-1}V_l', \qquad \text{on } \Gamma_d. \tag{5.15}$$

Using these known boundary conditions in equation (5.12), putting them on the right hand side and rearranging the coefficient matrices accordingly, we have

$$[RN]\begin{Bmatrix} \{\Phi_b\} \\ \{\partial\Phi_f/\partial\bar{n}\} \\ \{\partial\Phi_s/\partial\bar{n}\} \\ \{\Phi_d\} \end{Bmatrix}_e = [LN]\begin{Bmatrix} \{\partial\Phi_b/\partial\bar{n}\} \\ \{\Phi_f\} \\ \{\Phi_s\} \\ \{\partial\Phi_d/\partial\bar{n}\} \end{Bmatrix}_e \tag{5.16}$$

in which the subscript e is moved outside the braces and is replaced by an appropriate subscript symbolizing the corresponding part of the boundary, for the representations of Φ and $\partial\Phi/\partial\bar{n}$.

To get a relationship between $\{\Phi_d\}_e$ and $\{\partial\Phi_d/\partial\bar{n}\}_e$, let us first take the inverse of $[RN]$ such that

$$\begin{Bmatrix} \{\Phi_b\} \\ \{\partial\Phi_f/\partial\bar{n}\} \\ \{\partial\Phi_s/\partial\bar{n}\} \\ \{\Phi_d\} \end{Bmatrix}_e = [DD] \begin{Bmatrix} \{\partial\Phi_b/\partial\bar{n}\} \\ \{\Phi_f\} \\ \{\Phi_s\} \\ \{\partial\Phi_d/\partial\bar{n}\} \end{Bmatrix}_e$$

where

$$[DD] = [RN]^{-1}[LN].$$

Hence, expanding the above equation and noting equations (5.13)-(5.14), we have

$$\{\Phi_d\}_e = [EE]\left\{\frac{\partial\Phi_d}{\partial\bar{n}}\right\}_e \tag{5.17}$$

where $[EE]$ is a square submatrix of $[DD]$ which corresponds to $\{\partial\Phi_d/\partial\bar{n}\}_e$. Now let us assume that, according to the numbering rule of the interior domain, NL is the number of the node which is at the level of the upstream height; consequently, the orders of both $\{\Phi_d\}_e$ and $\{\partial\Phi_d/\partial\bar{n}\}_e$ are $NL \times 1$.

Prior to applying equation (5.15), we notice that in equation (5.17) the numbering of the nodes along the upstream interface needs to be reordered inversely such that it is consistent with that of the interior domain; thus, after doing this we have

$$\{\Phi_d\}_{(NL)\times 1} = [\tilde{EE}]_{(NL)\times(NL)}\left\{\frac{\partial\Phi_d}{\partial\bar{n}}\right\}_{(NL)\times 1}. \tag{5.18}$$

Applying equation (5.15) into (5.18), and using (4.32) and (4.36), we get

$$\begin{aligned} \{\Phi_d\}_{(NL)\times 1} &= [\tilde{EE}][TE]\,\bar{\omega}\begin{Bmatrix} 0 \\ \{v\} \end{Bmatrix} \\ &= \bar{\omega}\,[\tilde{PD}]_{(NL)\times(NL)}\begin{Bmatrix} 0 \\ \{v\} \end{Bmatrix}_{(NL)\times 1}. \end{aligned} \tag{5.19}$$

The above process is similar to the one described in obtaining equation (4.93). We notice the differences in sign between elements of $[TE]$ and those of $[TM]$ in equation (4.93).

Discretizing equation (5.11) along the interaction boundary, we can express the hydrodynamic pressure along the interface as

$$\{P\}_e = \overline{\omega}^2 \overline{\rho}\, [\tilde{PD}]_{(NL)\times(NL)} \begin{Bmatrix} 0 \\ \{v\} \end{Bmatrix}_{(NL)\times 1} . \tag{5.20}$$

The hydrodynamic pressure from the upstream harmonic water motion can then be taken into account by subtracting $[\tilde{PD}]$ in equation (4.20) from the first $(NL) \times (NL)$ elements of $[PD]$ in equation (4.94), while the rest of the elements in $[PD]$ are kept unchanged, and using this newly formulated $[PD]$ to implement the remaining calculations from equations (4.95)-(4.97).

5.3 Numerical Results

5.3.1 Computer Programming

A computer subroutine is written to incorporate the computations described in the preceding section. The equilibrium shape of the dam used for computation is non-symmetric because of the existence of upstream water; thus, the subroutine SYM described in Chapter 4 can not be used here.

The supplemental subroutine is comprised of the setting up of the boundary coordinates clockwise for the exterior domain according to the specified water height and the location of the imaginary boundary, and the use of the boundary element method to compute the matrix $[\tilde{PD}]$ in equation (4.20), which is needed for the representation of the exterior hydrodynamic pressure.

On the upstream membrane boundary, Γ_d, the membrane elements must be matched while calculating the pressures from both the interior and exterior domains, in order that $[\tilde{PD}]$ can be subtracted from the submatrix of $[PD]$ in equation (4.94); the specified exterior water height h_w, therefore, must be at the elevation of a node on the membrane. This causes an inconvenience if the results of a specified upstream water height are to be found; however, it can be achieved by scaling the results of two nodes nearest to that water level.

In our typical studies, the presence of two sharp corners on the membrane side of the exterior domain can considerably lessen the accuracy of results when using the boundary element method, because the convergence near these corners is slow [18]. This difficulty near the corners can be substantially diminished by the use of the double-node representation of corners, with each node located on a different boundary section. This approach is applied for all the corners in the exterior domain, while the one-node representation of the two corners is applied in the interior domain for the reason discussed in Subsection 4.5.1.

In addition, for clarity we use the same number of elements for Γ_f as for Γ_d, and the same for Γ_b as for Γ_s.

It should be observed that for some reasons the obtained λ may include a few negative or complex values, and have complex numbers for the higher modes. The latter may be similar to the ill-conditioned matrix approximations of the reduced wave integral equations [30]; the former may come from the damping effect of the exterior water motion. However, the first four λ values have no abrupt changes in values in figures presented later and are seen to be reliable.

A convergence test is performed to determine the appropriate location of the fictitious boundary and the fineness of the boundary element mesh, while the mesh for the interior domain is the same as that in Chapter 4. As shown in Table 5.1, the convergence is quickly achieved as the length of the base, XL, and the number of the elements of Γ_b, NI, increase. The values $NI = 50$ and $XL = 5.0$ are selected for our numerical calculations.

5.3.2 Results

The effects of various dimensionless parameters and the relative density are investigated numerically. Again, the first four eigenvalues λ, which are equal to the frequency squared, are studied against the other parameters. Typical natural vibration modes are illustrated in Fig. 5.2, and are seen to be tilted toward the downstream side.

Figs. 5.3-5.6 show the effects of h_w and h_i at the same time, while the membrane perimeter s_0, water elevation difference h_{iw}, i.e., $h_i - h_w$, and relative density $\overline{\rho}$ are fixed. At $\overline{\rho} = 1$, λ increases

NI	*XL*	λ_1	λ_2	λ_3	λ_4
10	2.0	0.3545	1.6938	4.9069	9.6772
20	3.0	0.3534	1.6923	4.9115	9.6719
30	3.0	0.3539	1.6938	4.9126	9.6727
40	4.0	0.3543	1.6945	4.9122	9.6737
50	4.0	0.3544	1.6948	4.9126	9.6738
50	5.0	0.3543	1.6946	4.9122	9.6739
60	5.0	0.3544	1.6948	4.9125	9.6739
70	6.0	0.3544	1.6948	4.9125	9.6739
70	7.0	0.3544	1.6947	4.9122	9.6739

Table 5.1 Test of Convergence Using $s_0 = 2.5$, $h_1 = 1.3121$, $h_w = 0.7131$, NL = 21, and $\bar{\rho} = 1$

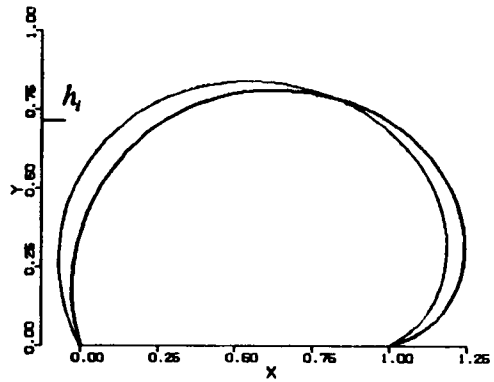

(a) First Mode

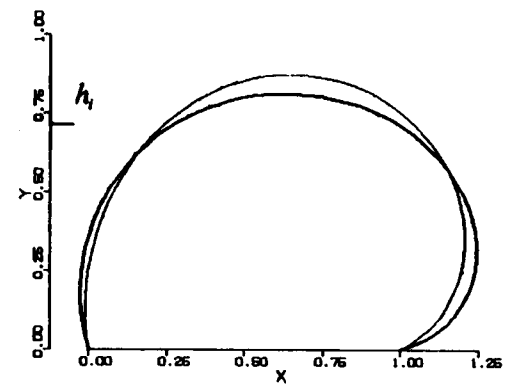

(b) Second Mode

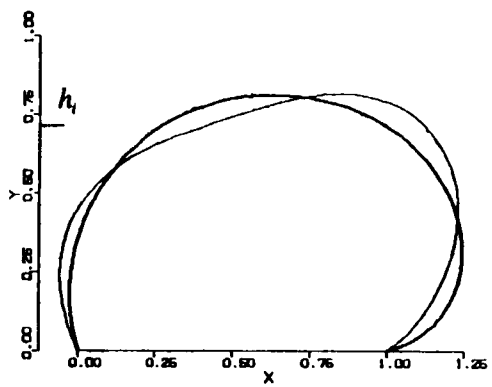

(c) Third Mode

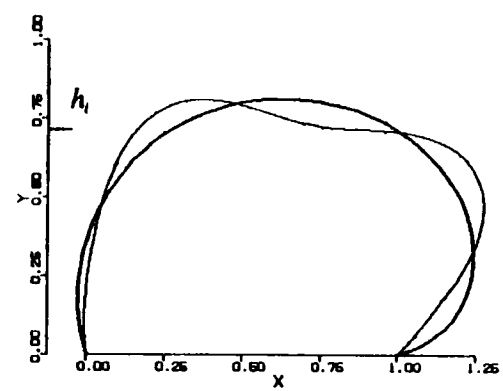

(d) Fourth Mode

Fig. 5.2 First Four Mode Shapes of Water-Inflated Membrane with an Upstream Head

almost linearly as h_w increases; at $\overline{\rho} = 100$, the third and fourth λ values increase significantly as h_w increases beyond 0.5.

The effect of the relative density is illustrated in Fig. 5.7 for $s_0 = 2.5$, $NL = 22$, and $h_{iw} = 0.75$. Similar results are seen in Figs. 4.9-4.10, for cases excluding the outside water.

Further, Figs. 5.8-5.9 show the effect of h_w, while keeping h_i fixed and $\overline{\rho} = 100$, for the two cases: (a) $s_0 = 2$, $h_i = 2.0$, (b) $s_0 = 4$, $h_i = 4.5$. Some of the values for these two figures are listed in Table 5.2. It is seen that λ decreases as h_w rises from 0 to about 0.5, and then the λ values may increase or decrease, as h_w continues to rise near the crest. However, the results of some investigations [29,31-33] showed that the natural frequencies become lower when some structures, e.g., plates or conical shells, vibrate in water. This disagreement may be attributed to the higher flexibility of the membrane, whose equilibrium shape changes significantly due to the existence of the outside water.

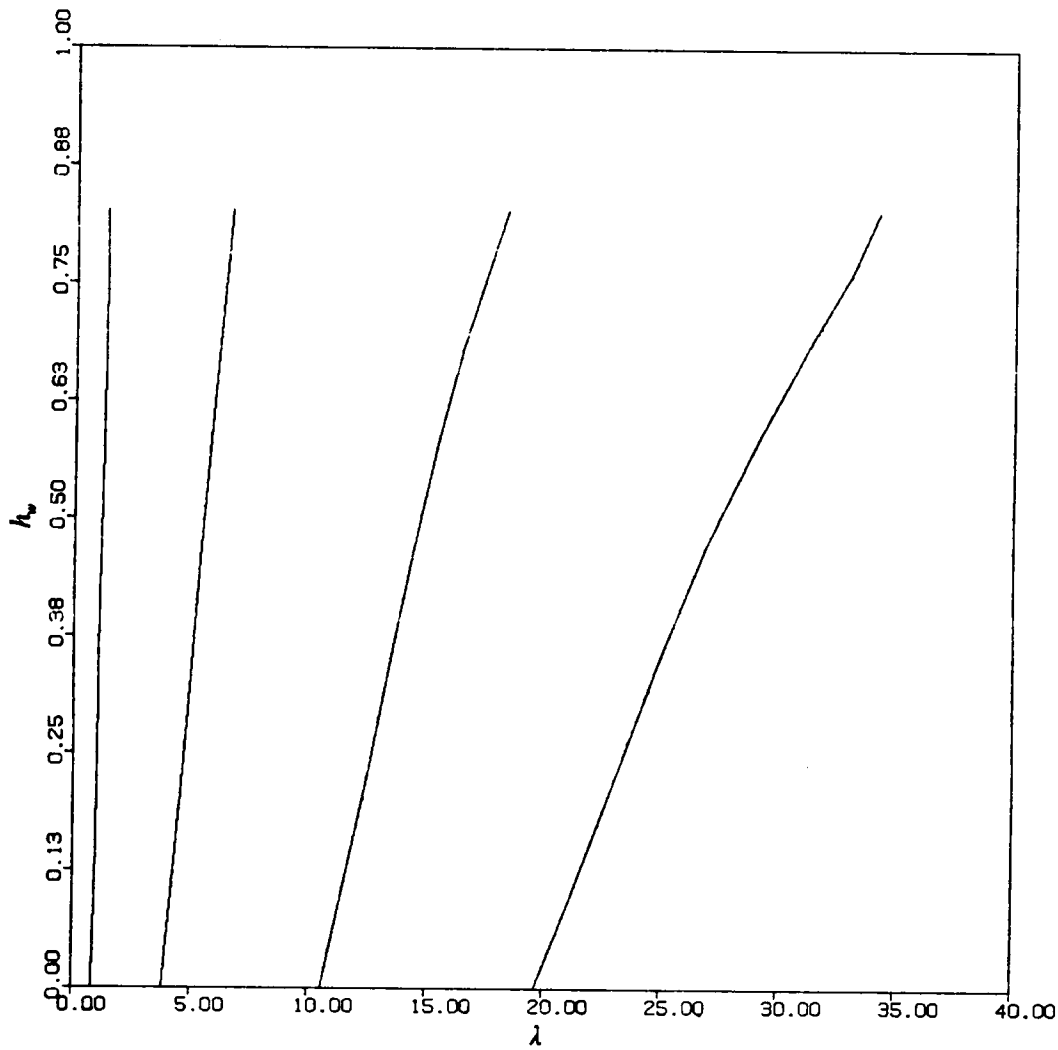

Fig. 5.3 h_w **vs.** λ **for** $s_0 = 2.5$, $h_{iw} = 2.0$, **and** $\bar{\rho} = 1.0$

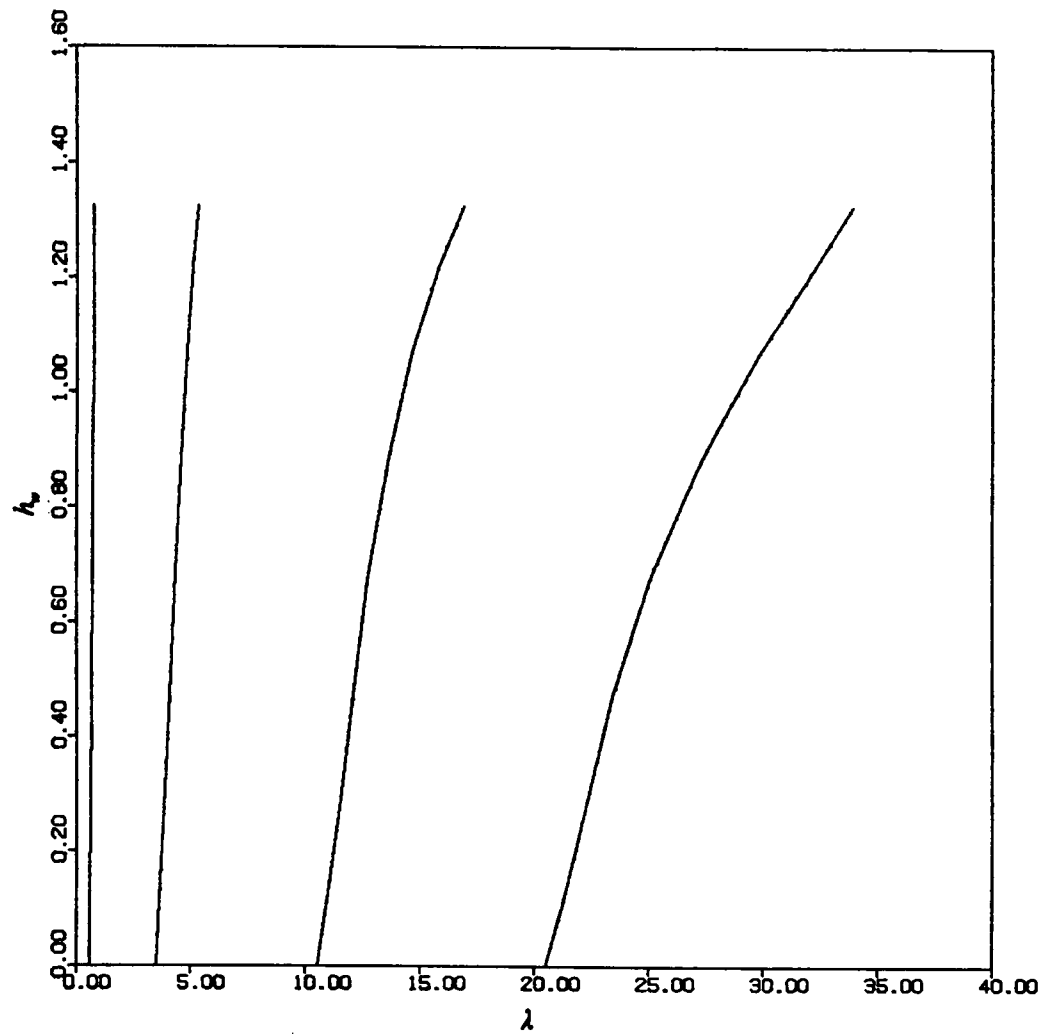

Fig. 5.4 h_w vs. λ for $s_0 = 4.0$, $h_{tw} = 4.0$, and $\bar{\rho} = 1.0$

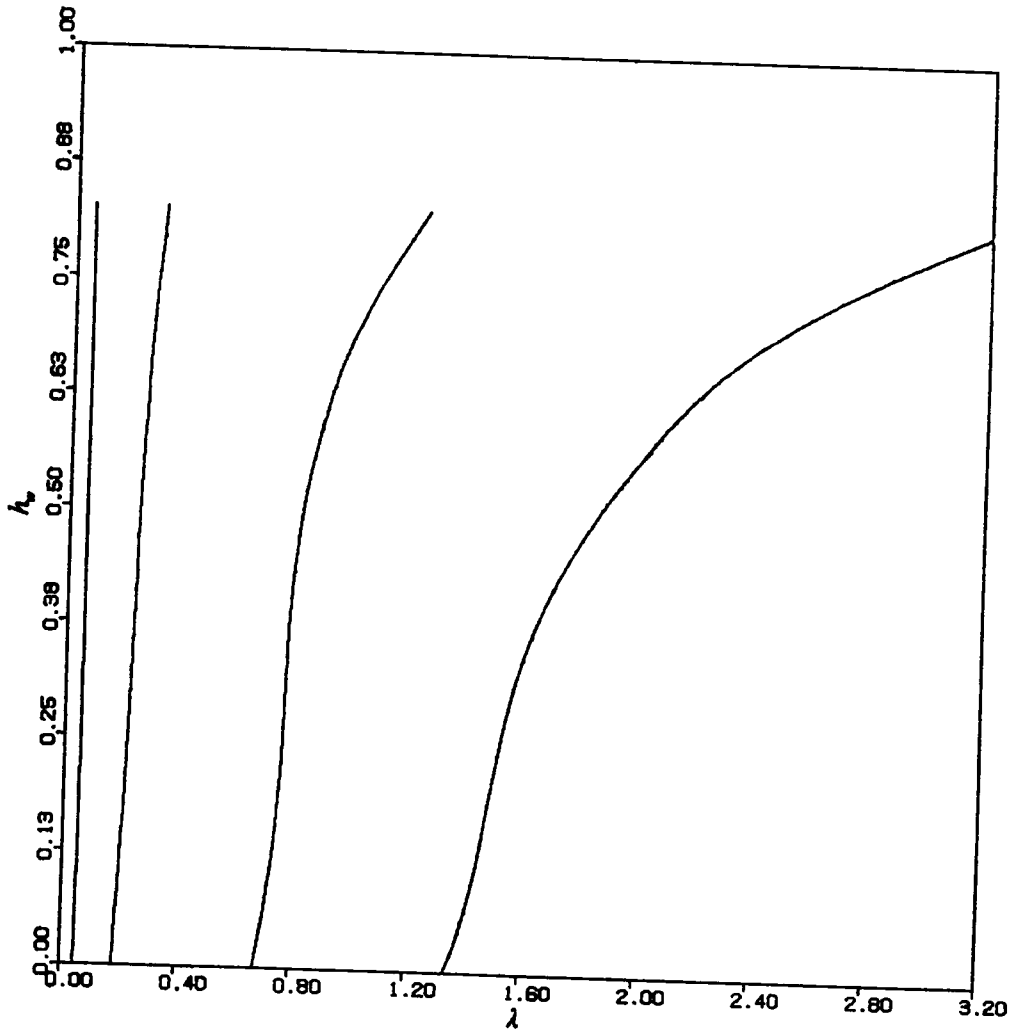

Fig. 5.5 h_w vs. λ for $s_0 = 4.0$, $h_l = 4.5$, and $\bar{\rho} = 100.0$

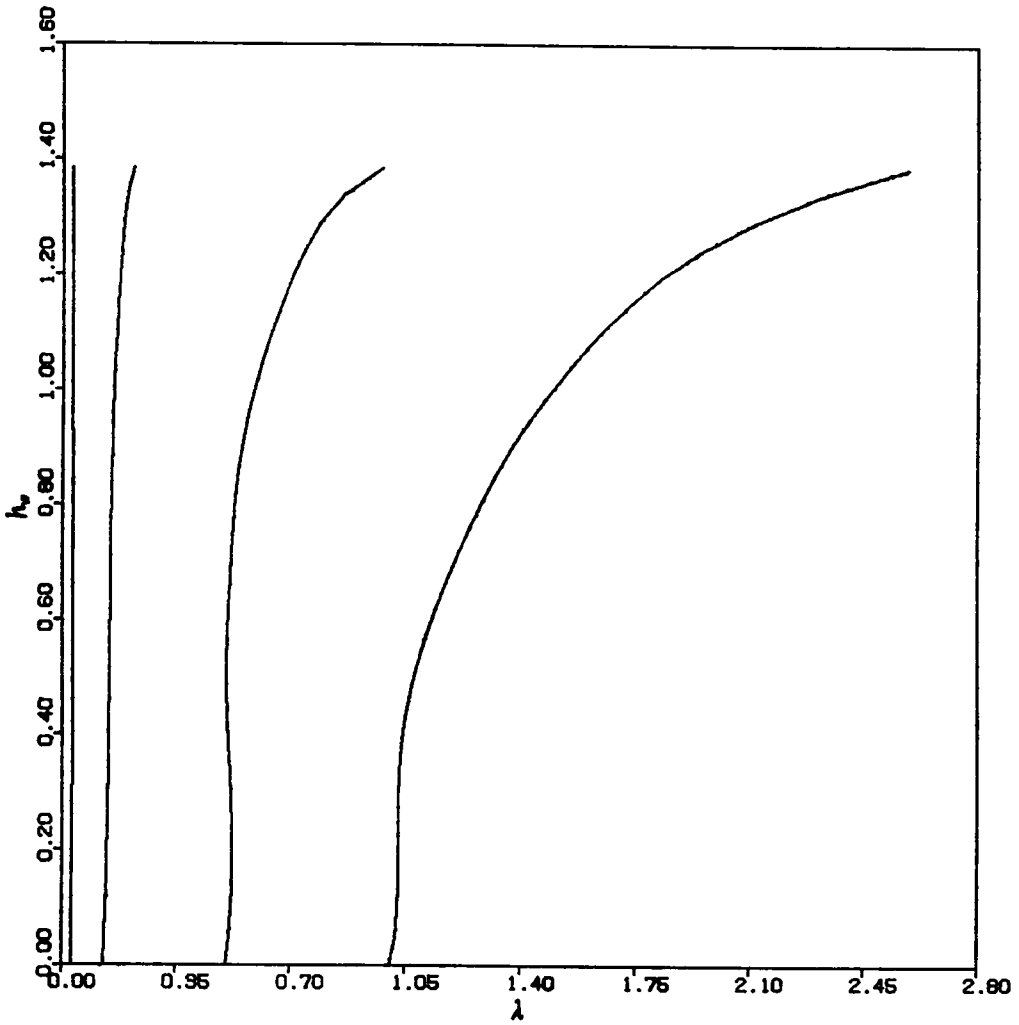

Fig. 5.6 h_w **vs.** λ **for** $s_0 = 4.0$, $h_{iw} = 2.0$,**and** $\bar{\rho} = 100.0$

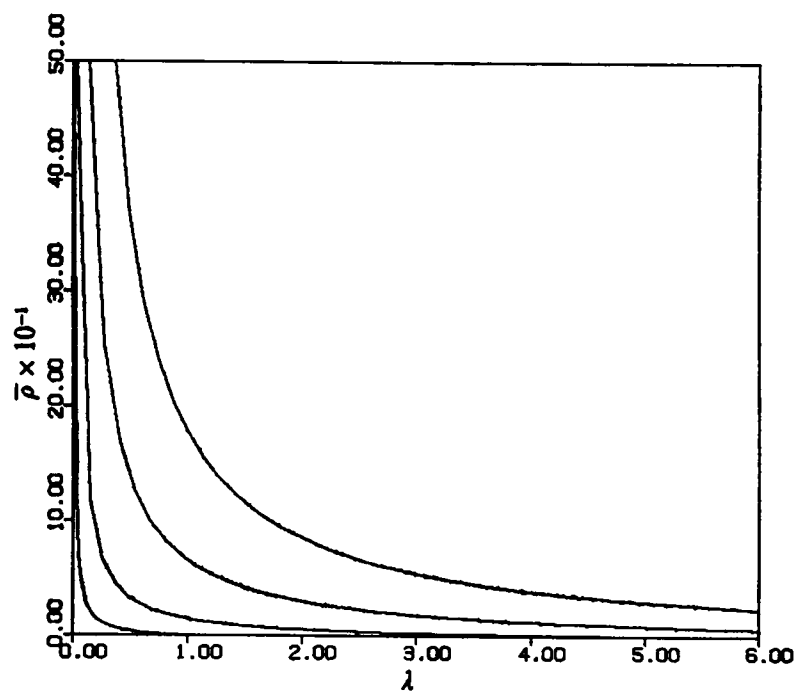

Fig. 5.7 $\bar{\rho}$ **vs.** λ **for** $s_0 = 2.5$, $h_u = 2.010$, $h_w = 1.260$

h_w	λ_1	λ_2	λ_3	λ_4
0.0	0.0478	0.1847	0.6800	1.3610
0.25	0.0471	0.1807	0.6404	1.2593
0.4	0.0453	0.1741	0.5757	1.2516
0.5	0.0434	0.1698	0.5631	1.3033
0.6	0.0410	0.1683	0.5773	1.4077
0.75	0.0369	0.1742	0.6580	1.6899
0.8	0.0354	0.1802	0.7135	1.8724

(a)

h_w	λ_1	λ_2	λ_3	λ_4
0.0	0.0327	0.1556	0.5950	1.1908
0.25	0.0324	0.1529	0.5606	1.1051
0.4	0.0317	0.1482	0.5135	1.0558
0.5	0.0311	0.1446	0.4910	1.0644
0.6	0.0303	0.1413	0.4784	1.0840
0.75	0.0290	0.1379	0.4771	1.1447
1.0	0.0265	0.1372	0.5114	1.2991

(b)

Table 5.2 The Effect of h_w on λ (a) for $s_0 = 2.5$, $h_1 = 2.0$, and $\bar{\rho} = 100.0$; (b) for $s_0 = 4.0$, $h_1 = 4.5$, and $\bar{\rho} = 100.0$

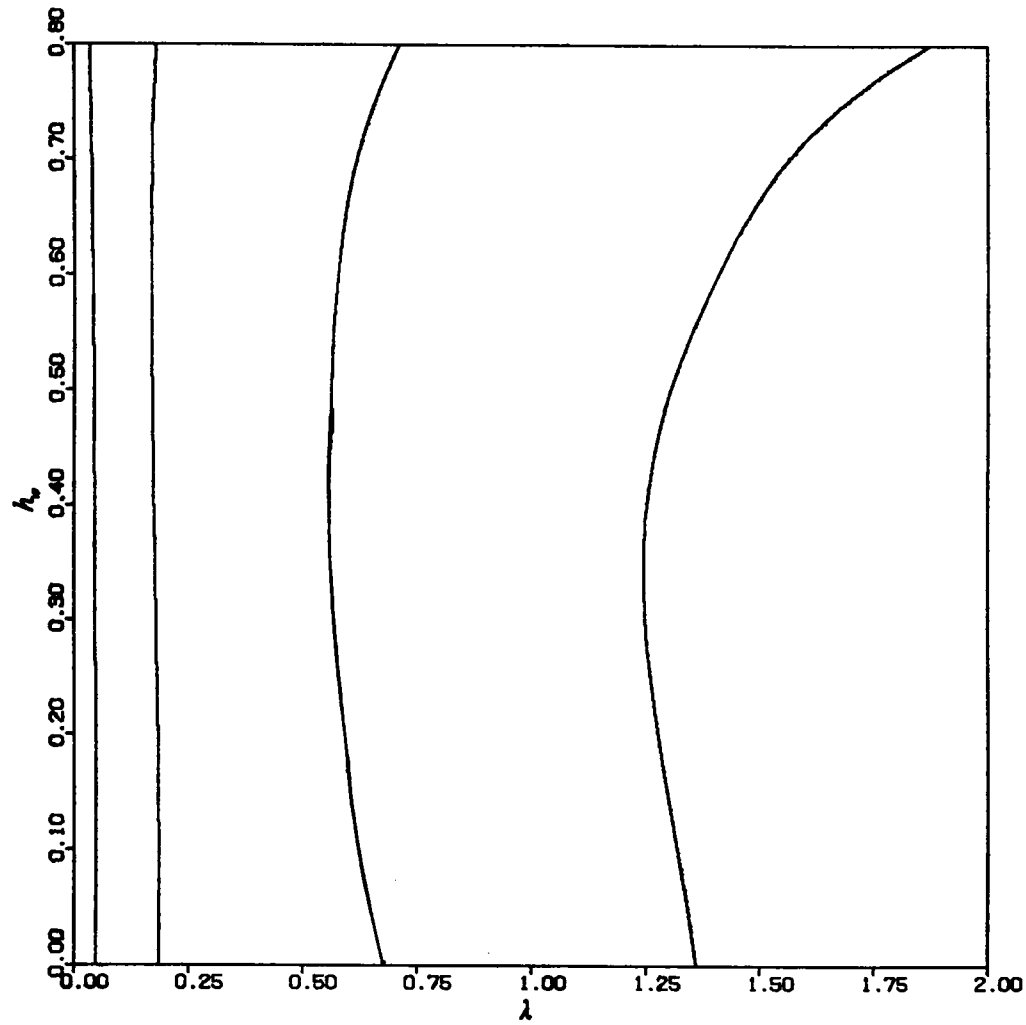

Fig. 5.8 h_w vs. λ for $s_0 = 2.5$, $h_i = 2.0$, and $\bar{\rho} = 100.0$

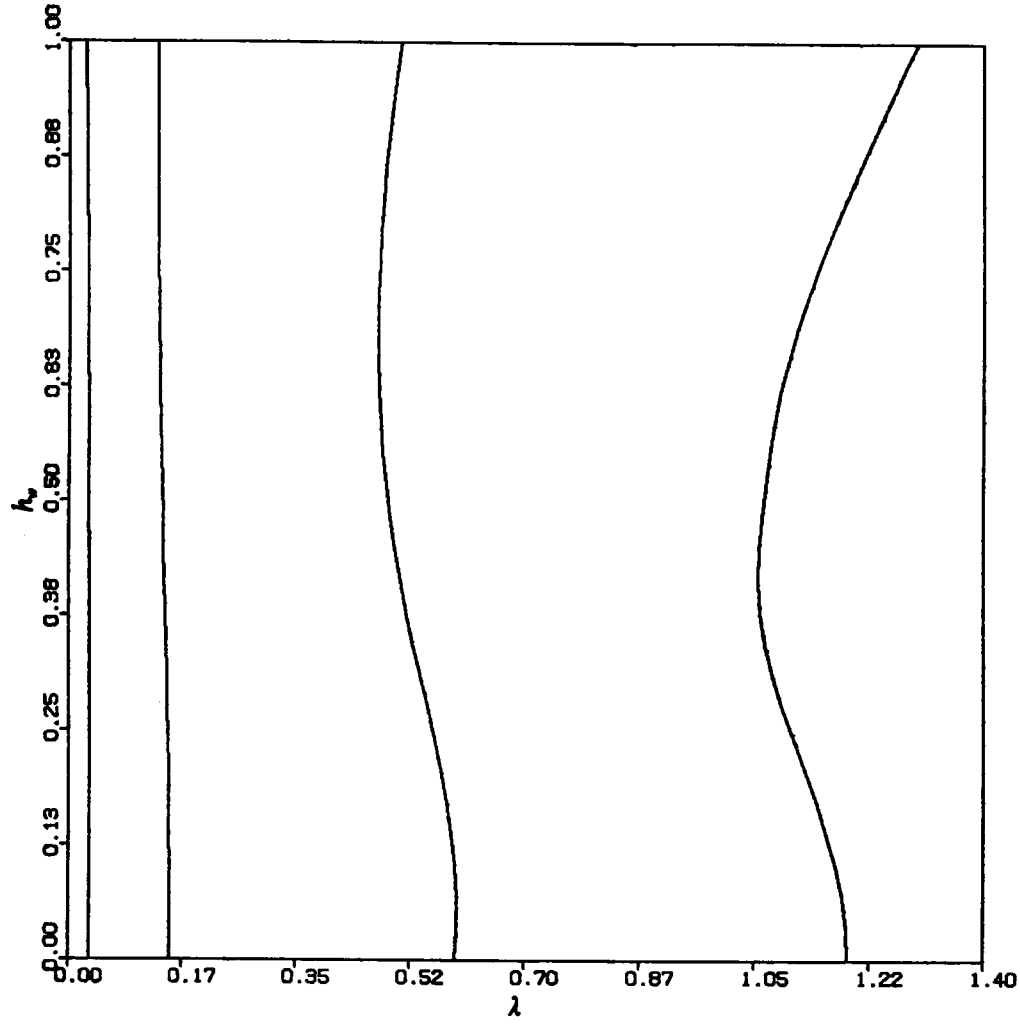

Fig. 5.9 h_w **vs.** λ **for** $s_0 = 4.0$, $h_i = 4.5$, **and** $\bar{\rho} = 100.0$

Chapter 6

CONCLUSION

6.1 Summary

This work deals primarily with the two-dimensional free vibrations of a water-inflated cylindrical membrane. The membrane equation of motion is derived and numerically solved using a finite difference method. The hydrodynamic pressure on the membrane is written in terms of the membrane displacements using a boundary integral equation method.

An effective iterative scheme, shooting $\psi_0(0)$ and t_0, is developed to find the equilibrium shape. For the membrane without water outside, the natural frequencies agree well with experimental values. The effect of the membrane mass is found to be insignificant. The eigenvalues increase almost linearly as the water head increases. The eigenvalues decrease as the ratio of the perimeter over base length increases, and become larger as the relative density of the water decreases.

For the membrane with an upstream water head, the free vibration modes are shown to be tilted toward the downstream side. In some typical illustrations, the eigenvalues ordinarily increase as the internal and upstream heads increase simultaneously, except when the internal head is low. The effect of the relative density is similar to the results of the case with no water outside. The existence

of the upstream head, while the internal head is kept fixed, affects the eigenvalues differently from the previous findings of other, stiffer, immersed structures; it is not always true that the existence of the outside water causes a drop in the lower eigenvalues in our study.

6.2 Recommendations for Further Studies

It is desirable to consider the compressibility of the fluid by solving a reduced wave integral equation and adding a radiation condition on the infinite water domain; thus, the impedance factor of the water motion can be examined. The surface wave may be included in calculating the exterior hydrodynamic pressure, but an expensive iterative scheme would be needed to find the eigenvalues. Also, the membrane behavior during earthquakes might be investigated.

The use of the finite element method in further studies to compute the hydrodynamic pressure may be considered. The programming of the boundary element method is highly problem dependent; on the other hand, existing finite element programs may be readily applied to the hydrodynamic analysis.

The behavior of the water-inflated dam under overflow conditions needs to be investigated. The fluctuation of the hydrodynamic pressure on the membrane during overflow may cause membrane collapse.

REFERENCES

1. Wang, C.-Y., "The Filling of a Long Membrane Container," *Journal of Structural Mechanics*, Vol. 12, No. 1, 1984, pp. 1-11.

2. Binnie, G. M., Thomas, A. R., and Gwyther, J. R., "Inflatable Weir Used During Construction of Mangla Dam," *Proceedings of the Institution of Civil Engineers, Part 1: Design and Construction*, Vol. 54, 1973, pp. 625-639; Discussion by C. van Beesten, Vol. 56, 1974, pp. 189-191.

3. "Report of an Investigation into the Failure of an Inflatable Dam," University of Sidney, Civil Engineering Laboratories, Investigation Report No. S89, May, 1969.

4. Firt, V., *Statics, Formfinding and Dynamics of Air-Supported Membrane Structures*, Martinus Nijhoff Publishers, The Hague, 1983, pp. 229-241.

5. Anwar, H. O., "Inflatable Dams," *Journal of the Hydraulics Division, American Society of Civil Engineers*, Vol. 93, May, 1967, pp. 99-118.

6. Binnie, A. M., "The Theory of Flexible Dams Inflated By Water Pressure," *Journal of Hydraulic Research*, Vol. 11, No. 1, 1973, pp. 61-68.

7. Irvine, H. M., *Cable Structures*, The MIT Press, Cambridge, Massachusetts, 1981, pp. 31-41.

8. Harrison, H. B., "The Analysis and Behavior of Inflatable Membrane Dams Under Static Loading," *Proceedings of the Institution of Civil Engineers*, Vol. 45, 1970, pp. 661-676; Closure, Vol. 48, 1971, pp. 137-139.

9. Parbery, R. D., "A Continuous Method of Analysis for the Inflatable Dam," *Proceedings of the Institution of Civil Engineers*, Part 2, Vol. 61, Dec., 1976, pp. 725-736.

10. Parbery, R. D., "Factors Affecting the Membrane Dam Inflated by Air Pressure," *Proceedings of the Institution of Civil Engineers*, Part 2, Vol. 65, Sept., 1978, pp. 645-654.

11. Hitch, N. M., and Narayanan, R., "Flexible Dams Inflated by Water," *Journal of Hydraulic Engineering*, ASCE, Vol. 109, No. 7, 1983, pp. 1044-1048.

12. Watson, R., "A Note on the Shapes of Flexible Dams," *Journal of Hydraulic Research*, Vol. 23, No. 2, 1985, pp. 179-194.

13. Fagan, T. D., "Effect of Membrane Weight on Vibrations of Air-Inflated Dams," *M.S. Thesis*, Virginia Polytechnic Institute and State University, Blacksburg, Virginia, 1987.

14. Leeuwrik, M. J., "Nonlinear Vibration Analysis of Inflatable Dams," *M.S. Thesis*, Virginia Polytechnic Institute and State University, Blacksburg, Virginia, 1987.

15. Baker, P. J., Buxton, D. H., and Worster, R. C., "Model Tests on a Proposed Flexible Fabric Dam for the Mangla Project, Pakistan, Parts I and II," *The British Hydromechanics Research Association*, Reports RR 803 and 827, February, 1965.

16. Henrych, J., *The Dynamics of Arches and Frames*, Elsevier Scientific Publishing Company, Amsterdam, 1981, pp. 21-27.

17. Forsythe, G. E., Malcolm, M. A., and Moler, C. B., *Computer Methods for Mathematical Computations*, Prentice-Hall, Englewood Cliffs, New Jersey, 1977, pp. 156-166.

18. Brebbia, C. A., *The Boundary Element Method for Engineers*, Pentech Press, London, 1978.

19. Banerjee, P. K., and Butterfield, R., *Boundary Element Methods in Engineering Sciences*, McGraw-Hill Book Company (UK) Limited, London, 1981.

20. Lamb, H., *Hydrodynamics*, Dover Publications, 6th edition, New York, 1932, pp. 19-20.

21. Fairweather, G., Rizzo, F. J., Shippy, D. J., and Wu, Y. S., "On the Numerical Solution of Two-Dimensional Potential Problems by an Improved Boundary Integral Equation Method," *Journal of Computational Physics*, Vol. 31, 1979, pp. 96-112.

22. Ingham, D. B., Heggs, P. J., and Manzoor, M., "Boundary Integral Equation Solution of Nonlinear Plane Potential Problems," *IMA Journal of Numerical Analysis*, Vol. 1, 1981, pp. 415-426.

23. Jaswon, M. A., and Symm, G. T., *Integral Equation Methods in Potential Theory and Elastostatics*, Academic Press, New York, 1977, pp. 143-149.

24. Liggett, J. A., and Liu, P. L.-F., *The Boundary Integral Equation Method for Porous Media Flow*, George Allen & Unwin, London, 1983.

25. Ting, A.-L., and Liu, P. L.-F., "Boundary Integral Solutions for Nonlinear Forces on Objects Beneath Waves," *Innovative Numerical Methods in Engineering*, 4th International Symposium, 1986, pp. 619-625.

26. Liu, P. L.-F, and Cheng, A. H.-D., "Boundary Solution for Fluid-Structure Interaction," *Journal of Hydraulic Engineering* , ASCE, Vol. 110, No. 1, 1984, pp. 51-64.

27. Liu, P. L.-F., "Hydrodynamic Pressures on Rigid Dams During Earthquake," *Journal of Fluid Mechanics*, Vol. 165, 1986, pp. 131-145.

28. Hanna, Y. G., and Humar, J. L., "Boundary Element Analysis of Fluid Domain," *Journal of the Engineering Mechanics Division*, Proceedings of ASCE, Vol. 108, No. 2, 1982, pp. 436-449.

29. Shingu, K., and Nishimura T., "A Study on Dynamic Response of Submerged Conical Shells," *Shells, Membranes and Space Frames*, Proceedings of IASS Symposium, Edited by K. Heki, Vol. 1, Osaka, 1986, pp. 81-88.

30. Mathews, I. C., "Numerical Techniques for Three-Dimensional Steady-State Fluid-Structure Interaction," *Journal of the Acoustical Society of America*, Vol. 79, No. 5, 1986, pp. 1317-1325.

31. De Espinosa, F. M., and Gallego-Juarez, J. A., "On the Resonance Frequencies of Water-Loaded Circular Plates," *Journal of Sound and Vibration*, Vol. 94, No. 2, 1984, pp. 217-222.

32. Muthuveerappan, G., Ganesan, N., and Veluswami, M. A., "Vibrations of Skew Plates Immersed in Water," *Computers and Structures*, Vol. 21, No. 3, 1985, pp. 479-491.

33. Nagaya, K., and Takeuchi, J., "Vibration of a Plate with Arbitrary Shape in Contact with a Fluid," *Journal of the Acoustical Society of America*, Vol. 75, No. 5, 1985, pp. 1511-1518.

The vita has been removed from the scanned document